# Finite Activity Jump Models For Option Pricing

Mercy Muthoni Koimburi

Supervisor
Prof. Ronald Becker

Dissertation

in partial fulfillment of the requirements of the degree of
MSc In Financial Mathematics
University of Cape Town

April 2011

**Acknowledgements**

I would like to express my gratitude to my supervisor, Prof. Ronald Becker, for his assistance and direction throughout this paper. I am also thankful to my family and friends, for their prayers and continual encouragment. A special thanks to my husband, Felix Njenga Koimburi, whose love, support and editing assistance has been invaluable. Thank you for encouraging me to persevere. Above all, thanks be to God who gives us the strength.

# Contents

**Abstract**

This thesis aims to look at option pricing under affine jump diffusion processes, with particular emphasis on using Fourier transforms. The focus of the thesis is on using Fourier transform to price European options and Barrier options under the Heston stochastic volatility model and the Bates model. Bates model combines Merton's jump diffusion model and Heston's stochastic volatility model. We look at the calibration problem and use Matlab functions to model the DAX options volatility surface. Finally, using the parameters generated, we use the two stated models to price barrier options.

# 1 Introduction

Options are a type of derivative, which are contracts based on an underlying asset. A stock is an example of an asset. There are two main types of options, namely a call and a put option. A call option gives the holder the right, but not the obligation, to buy an underlying asset by a certain future date at a certain price. While a put option allows the holder to sell this asset at a future date at a certain price, under the same conditions. The future date is known as the expiration date or maturity and the specified price is called the exercise or strike price. If an option can only be exercised at the expiration date, then it is called a European option. If the right to buy or sell an underlying asset can be exercised at any time up to the expiration date, then the option is called an American option. The value of an option when it is exercised is called its payoff. Given a particular stochastic differential equation, of a given model, one can then fit the coefficient parameters using market prices of puts and calls, and then price exotics using Monte Carlo. In this paper we will consider the pricing of European call and put options using various models. We will then go on to price specifically barrier options using Monte Carlo. A barrier option is a path-dependent option whose pay-off at maturity depends on whether or not the underlying spot price has crossed some pre-defined barrier value during the life of the option.

Options or derivatives are widely used by individuals and companies who wish to buy or sell assets in advance to insure themselves against market movements, while others enter into these contracts for speculative purposes. It then becomes important to have adequate pricing models to calculate fair prices for these financial contracts which are derived from some underlying asset. Given a particular model, every option has its calculated value and a market price. The former is obtained using the pricing model. The pricing model usually makes assumptions about the distribution of the underlying asset and proposes a hedging strategy to replicate the option payoff. Thus an ideal pricing model leads to a good replication of the option payoff at maturity. The market value, on the other hand, is the amount of money needed to acquire this option [2].

Many models used in derivative pricing assume that the underlying asset follows continuous sample paths as is given by the Black Scholes SDE with constant drift and diffusion parameters.

$$dS_t = (r - d)S_t dt + \sigma S_t dW_t \tag{1.1}$$

where $S_t$ is the asset (underlying) price, and $r$, $d$, $\sigma$ are constants. $r$ is the risk free interest rate, $d$ is the dividend rate, $\sigma$ is the volatility, $W_t$ is a standard Wiener process.

Volatility in the market measures the uncertainty associated with the asset price. The Black Scholes model assumes that this volatility is constant. Volatility can be estimated as the standard deviation of expected returns on a security/asset over a given period of time. Alternatively it can be calculated from option prices observed in the market. When calculated using the latter method, it is referred to as the Black Scholes implied volatility $\sigma_{imp}$ and is the solution to

$$F_{BS}(S, t, \sigma_{imp}(K, T); K, T) = F_{market}(S, t; K, T) \tag{1.2}$$

where $F_{BS}(\sigma_{imp}(K, T); K, T)$ is the Black Scholes price with $\sigma = \sigma_{imp}$ and $F_{market}(K, T)$ is the market price of a vanilla option with strike $K$ and expiry $T$.

The volatility smile is then the plot of market implied volatilities versus strike for a given constant expiration time and initial value. The term structure of the implied volatility is the plot of market implied volatilities for at-the-money options versus maturities. Together, these two features produce the volatility surface where market implied volatilities are plotted across all possible strikes and maturities. Given that the Black Scholes model assumes volatility is constant, the volatility surface is in turn flat across all strikes and maturities. However, in reality, option markets exhibit the volatility smile phenomenon which means that the surface is not flat as expected in the Black Scholes model, but rather it has some curvature.

Studies have been undertaken to try and explain one or all of the phenomena described above. Some of the popular models include: a) The jump diffusion models of Merton [23], and Kou [22]; b) The constant elasticity of variance model of Cox and Ross [9]; c) The stochastic volatility models of Hull and White [19], Stein and Stein [28] and Heston [17]; d) The stochastic volatility jump diffusion models of Bates [3] and Scott [26]. Most of these models look at modifying the asset price dynamics by introducing price-jumps, stochastic volatility or a combination of both to explain the above observed phenomena. Importantly it has been observed that introducing stochastic volatility is necessary to calibrate the longer maturities, while jumps reflect shorter maturity option pricing. Furthermore, the logarithm of a price process that follows jumps is leptokurtic, as observed by the high peaks and heavy tails, phenomena that are evident in market data. This paper focuses on using Fourier transform methods to price European options under Heston's stochastic volatility model, Merton's jump diffusion model and the Bates model, and the impact they each have on the volatility smile.

The paper is structured as follows: Chapter 2 gives background information on the Black Scholes pricing model. It then briefly outlines the Poisson process which is a fundamental building block of jump diffusion, before ending off with a discussion on Fourier transforms. The stochastic volatility model as introduced by Heston and derivation of its characteristic function is addressed in chapter 3. In this chapter we present pricing of European options using Fourier transform by means of quadrature integration techniques and also present the Fourier-cosine expansion method as an alternative method. Chapter 4 explores jump diffusion. This chapter also covers the derivation of the characteristic function of the Bates model, which incorporates both price-jumps and stochastic volatility. Chapter 5 discusses barrier option pricing, while chapter 6 deals with the calibration problem and uses the implied volatility of the DAX (The Deutscher Aktienindex) vanilla options to specify parameters best fit to use in our model. The implementation and numerical results of the models stated above, namely Heston's stochastic volatility model and Bates model are then considered in chapter 7. It is here that we use Monte Carlo simulations to compare barrier option prices generated using the Heston, Bates model and Black Scholes model and also barrier options generated using a binomial tree. The conclusions drawn from the results of this thesis are laid out in the chapter 8.

# 2 Motivation and Parameters

## 2.1 Black Scholes Model

Let $S_t$ be the stock price at time $t$, $\mu$ the expected rate of return on $S_t$ and $\sigma$ the volatility of $S_t$. The dynamics of the stock price $S_t$ is assumed to be

$$dS_t = \mu S_t dt + \sigma S_t dW_t \tag{2.1}$$

where $W_t$ is a standard Brownian motion. By Ito's lemma we derive the Black Scholes partial differential equation (PDE). The full derivation can be found in Appendix A

$$\frac{\partial V}{\partial t} + \frac{1}{2}\sigma^2 S^2 \frac{\partial^2 V}{\partial S^2} + rS\frac{\partial V}{\partial S} - rV = 0 \tag{2.2}$$

Two ways of deriving Black Scholes formula are outlined below: The first comes about by solving the differential equation, while the second approach involves using the risk-neutral valuation.

### 2.1.1 Partial Differential Equation

The Black Scholes PDE does not have a unique solution, but the unique price for a particular derivative can be obtained by solving the PDE subject to the derivative's boundary condition. In the case of a European option, the boundary condition is the payoff function at the expiration of the option. Let $C(S_t, t)$ be the value of a European call option and $P(S_t, t)$ the European put at times $t$. Then the payoff at time $T$ is $C(S_T, T) = \max(S_T - K, 0)$ and $P(S_T, T) = \max(K - S_T, 0)$ respectively. Replacing $V(S_t, t)$ by $C(S_t, t)$ and solving the PDE subject to the boundary conditions gives

$$C = S_0 N(d_1) - Ke^{-rT} N(d_2) \tag{2.3}$$

and

$$P = Ke^{-rT} N(-d_2) - S_0 N(-d_1) \tag{2.4}$$

where

$$d_1 = \frac{\ln(S_0/K) + (r + \sigma^2/2)T}{\sigma\sqrt{T}} \tag{2.5}$$

$$\begin{aligned} d_2 &= \frac{\ln(S_0/K) + (r - \sigma^2/2)T}{\sigma\sqrt{T}} \\ &= d_1 - \sigma\sqrt{T} \end{aligned} \tag{2.6}$$

where $r$ is a risk free interest rate. The function $N(x)$ is the cumulative probability distribution function for a standardized normal distribution. The put option price is derived by the put-call parity which is given by

$$c + Ke^{-r(T-t)} = p + S_t \tag{2.7}$$

where $c$ is the call price and $p$ the put price.

### 2.1.2 Risk Neutral Evaluation

Option Pricing is done using the concept of no arbitrage. This states that there is never any opportunity to make a risk-free profit. More correctly, such opportunities cannot exist for a significant length of time before prices move to eliminate them. Almost all financial theories assume the existence of risk-free investments that give a guaranteed return with little chance of default. A government bond or a deposit in a sound bank are examples of two such investments. This implies that, the greatest risk-free return that one can make on a portfolio of assets is the same as the return if the equivalent amount of cash were placed in a bank. As such if one wants a greater return, one must accept a greater risk. The arbitrage theory leads to the definition of the risk-neutral world.

The risk-neutral world assumes that all investors are risk neutral, that is, investors do not expect any extra returns by taking on additional risk. The expected return is the same regardless of the risk involved and is considered to be the risk-free rate of interest $r$ [19].

Thus consider a derivative that provides a payoff at one particular time. It can be valued using risk-neutral valuation by using the following procedure as given in Hull [19]

1. Assume that in a risk-neutral world, the expected return on any asset is the risk-free interest rate $r$. This implies that, under risk-neutral valuation, $\mu = r$ for the stock price of a non-dividend paying stock that follows the process of equation( 2.1). That is,

$$dS_t = rS_t dt + \sigma S_t dW_t \tag{2.8}$$

2. Next, calculate the expected payoff from the derivative. For a call option this would be

$$\mathbb{E}[\max(S_t - K, 0)] \tag{2.9}$$

where $\mathbb{E}$ is the expected value in a risk-neutral world.

3. Discount the expected payoff at the risk-free interest rate, which would be depicted as given below for a call option

$$C = e^{-rT}\mathbb{E}[\max(S_T - K, 0)] \tag{2.10}$$

where it can be shown that

$$C = e^{-rT}[S_0 N(d_1)e^{rT} - KN(d_2)] \tag{2.11}$$

## 2.2 Poisson Processes

The fundamental jump process is either the Poisson process or the compound Poisson process, with the only difference being that the compound Poisson process has jumps of random sizes. Models based on Levy processes are also used. For models of financial markets, we need to allow the jump size to be random. Hence in this thesis we use the compound Poisson process. In this section we will look at the Poisson process and some of its properties, since these processes serve as the building blocks for the jump processes.

### 2.2.1 The Poisson Process

Take a sequence $\{\tau_i\}_{i\geq 1}$ of independent exponential random variables with parameter $\lambda$, that is, with cumulative distribution function $P[\tau_i \geq y] = e^{-\lambda y}$. The Poisson process models an event, which we call a "jump", that occurs from time to time, such that

$$G_n = \sum_{i=1}^{n} \tau_i \tag{2.12}$$

where $G_n$ is the time of the $n$th jump.
The Poisson process $N(t)$ counts the number of jumps that occur at or before time $t$. We define a Poisson process to be the process of the form

$$N(t) = \sum_{n\geq 1} 1_{\tau_n} \quad (S_n \leq t, t > 0) \tag{2.13}$$

If we suppose that $N_0 = 0$, then $N(t)$ is the number of jumps which are observed to have occurred in the interval [0, t]. Because the expected time between the jumps is $\frac{1}{\lambda}$, the jumps are arriving at an average rate of $\lambda$. Hence $N(t)$ is a Poisson random variable with mean $\lambda$t, with $\lambda$ being called the *intensity*.

The Poisson process, like Brownian motion, has the very important properties of independence and stationarity of increments. That is, for every $t > s$ the increment $N(t) - N(s)$ is independent of the history of the process up to and including time $s$ and has the same distribution as $N(t - s)$.

### 2.2.2 Compound Poisson Process

Suppose we are given $N(t)$, a Poisson process with intensity $\lambda$, and $\{Y_i\}_{i\geq 1}$, a sequence of independent and identically distributed random variables. We assume the random variables $Y_i$ are independent of each other and of the Poisson process $N(t)$. We then define the compound Poisson process as

$$Q(t) = \sum_{i=1}^{N(t)} Y_i \quad t \geq 0 \tag{2.14}$$

In this case the jumps in $Q(t)$ occur at the same time as the jumps in $N(t)$. While the jumps in N(t) in a Poisson process are always of size 1, those in $Q(t)$ are of a random size.

## 2.3 Fourier Transform

The Fourier transform ($\mathcal{F}\{\cdot\}$) and the inverse Fourier transform ($\mathcal{F}^{-1}\{\cdot\}$) of an integrable function, $g(x)$ is given by

$$\mathcal{F}\{g(x)\} = \int_{-\infty}^{+\infty} e^{iux} g(x)dx = G(u) \quad u \in \mathbb{R} \tag{2.15}$$

$$\mathcal{F}^{-1}\{G(u)\} = \frac{1}{2\pi}\int_{-\infty}^{+\infty} e^{-iux} G(u)du = g(x) \tag{2.16}$$

In order to recover the function $G(u)$ from the Fourier transform we apply the inverse Fourier transform.

For a random variable $X$ the characteristic function can be expressed as follows

$$\begin{aligned} \phi(u) &= \mathbb{E}[e^{iuX}] \\ &= \int_{-\infty}^{\infty} e^{iux} f(X)dX \end{aligned} \tag{2.17}$$

where $f(X)$ is the probability density function of $X$. We use these relationships in chapter 3 for option pricing under the Heston Stochastic model.

# 3 Stochastic Volatility Models

This section looks specifically at Heston's model that, unlike the Black Scholes model, assumes that volatility is stochastic. In reality the volatility process cannot be directly observed. However, empirical studies have shown that the estimated volatility seems to fluctuate around a mean value.

Many models that assume stochastic volatility have been proposed, such as those by Hull White (1987)[19], Stein-Stein (1991)[28], Scott (1997)[26], Schobel and Zhu (1998)[29] and Heston (1993)[17]. These models show that introducing stochastic volatility in the stock price explains in a consistent way why options with different strikes and expirations have different Black Scholes implied volatility.

We give a table of the different dynamics that have been introduced in stochastic volatility models, and then focus on the Heston stochastic volatility model.

| Stochastic Volatility Models | |
|---|---|
| Hull White | $ds = \mu_s S dt + \sqrt{\nu} S dW_s$<br>$d\nu = \mu_\nu \nu dt + \xi \nu dW_\sigma$<br>$dW_s \cdot dW_\sigma = \rho dt$ |
| Scott | $ds = \mu S dt + e^y S dW_s$<br>$dy = \kappa(\theta - y)dt + \alpha dW_y$<br>$dW_s \cdot dW_y = \rho dt$ |
| Stein | $ds = \mu S dt + \sigma S dW_s$<br>$d\sigma = \kappa(\theta - \sigma)dt + \alpha dW_\sigma$<br>$dW_s \cdot dW_\sigma = \rho dt$ |
| Heston | $ds = \mu S dt + \sqrt{\nu} S dW_s$<br>$d\nu = \kappa(\theta - \nu)dt + \alpha\sqrt{\nu} dW_\nu$<br>$dW_s \cdot dW_\nu = \rho dt$ |

## 3.1 Heston's Model

The Heston stochastic volatility model models the variance as a square root process that is correlated with the stock price. The model is based on the following equations which represent the dynamics of the stock price and the variance processes under risk neutral measure:

$$dS = rSdt + \sqrt{V_t}SdW_t \tag{3.1}$$

$$dV_t = \kappa(\theta - V_t)dt + \sigma_v\sqrt{V_t}dZ_t \tag{3.2}$$

$$dZ_t = \rho dW_t + \sqrt{1-\rho^2}dW_t^1 \tag{3.3}$$

The first equation gives dynamics of the stock price $S$ at time $t$, with $r$ being the risk neutral drift, and $\sqrt{V_t}$ being the volatility of the underlying asset. The second equation then gives the evolution of the variance process which follows a square-root process, where $\theta$, $\kappa$ and $\sigma_v$ are constants and

- $\theta$ is the long-term mean of the variance
- $\kappa$ is the rate of mean reversion
- $\sigma_v$ is the parameter which determines the volatility of the variance process.
- $W_t$ and $W_t^1$ are independent Brownian motion processes.

In equation (3.2), if we set $\kappa$ and $\theta$ to be positive, the drift of the volatility will decrease as the volatility increases and vice versa. This property ensures that the volatility does not increase without limitation. Furthermore, the volatility process has a zero probability of attaining a zero value if $\kappa\theta - \frac{1}{2}\sigma^2 \leq 0$ is fulfilled.

### 3.1.1 Heston Closed Form Solution

Heston proposed a method to price European call options in stochastic volatility models. We give this solution below. More details can be found in Heston (1993)[17].

By applying Ito's Lemma and the arbitrage theory as shown in Appendix B, any asset $V(S,\nu,t)$ satisfying the Heston model must satisfy the following PDE

$$\frac{\partial V}{\partial t} + \frac{1}{2}\nu S^2\frac{\partial^2 V}{\partial S^2} + \rho\sigma\nu S\frac{\partial^2 V}{\partial S\partial\nu} + \frac{1}{2}\sigma^2\nu\frac{\partial^2 V}{\partial\nu^2} + (rS)\frac{\partial V}{\partial S} + (\kappa(\theta-\nu_t))\frac{\partial V}{\partial\nu} - rV = 0 \tag{3.4}$$

Before solving equation (3.4) with the appropriate boundary conditions, we can simplify it by making some suitable changes of variables. Let $K$ be the strike price of the option, $T$ time to expiration, $F_{t,T}$ the time $T$ forward price of the stock index and $x := \log(F_{t,T}/K)$.

Further, suppose that we consider only the future value to expiration $C$ of the European option price rather than its value today and define $\tau = T - t$, Then the equation (3.4) simplifies to

$$-\frac{\partial C}{\partial \tau} + \frac{1}{2}\nu C_{11} - \frac{1}{2}\nu C_1 + \frac{1}{2}\eta^2 \nu C_{22} + \rho\eta\nu C_{12} + \kappa(\theta - \nu)C_2 = 0 \tag{3.5}$$

where the subscripts 1 and 2 refer to differentiation with respect to $x$ and $\nu$ respectively.

According to Duffie, Pan and Singleton [12] the closed form solution of a European call option for the Heston model has the following form:

$$\begin{aligned} C &= e^{-r\tau}\mathbb{E}\Big[(S_T - K)^+\Big] \\ &= e^{-r\tau}\mathbb{E}[S_T 1_{S_T>K}] - e^{-r\tau}K\mathbb{E}[1_{S_T>K}] \\ &= K\Big\{e^x P_1(x,\nu,\tau) - P_0(x,\nu,\tau)\Big\} \end{aligned} \tag{3.6}$$

In this expression $P_j(x, \nu, \tau)$ each represent the probability of the call expiring in-the-money, conditional on the value $x := \log(F_{t,T}/K)$ of the stock and on the value $\nu_t$ of the volatility at time $t$, where $\tau = T - t$ is the time to expiration. We follow closely results as given by Gatheral [21] to solve equation (3.4). Substituting equation (3.6) into equation (3.4) implies that $P_j(x, \nu, \tau)$ must satisfy the equation .

$$-\frac{\partial P_j}{\partial \tau} + \frac{1}{2}\nu\frac{\partial^2 P_j}{\partial x^2} - (\frac{1}{2} - j)\nu\frac{\partial P_j}{\partial x} + \frac{1}{2}\sigma^2\nu\frac{\partial^2 P_j}{\partial \nu^2} + \rho\sigma\nu\frac{\partial^2 P_j}{\partial x \partial v} + (a - b_j\nu)\frac{\partial P_j}{\partial \nu} = 0 \tag{3.7}$$

where $\tau = T - t$, $j = 0, 1$ and

$$a = \kappa\theta \tag{3.8}$$

$$b_j = \kappa - j\rho\sigma \tag{3.9}$$

subject to the terminal condition

$$\lim_{\tau\to\infty} P_j(x,\nu,\tau) = \begin{cases} 1 & \text{if} \quad x > 0 \\ 0 & \text{if} \quad x \leq 0 \end{cases}$$

We solve equation (3.7) using a Fourier transform. To this end equation (3.7) becomes

$$\int_{-\infty}^{\infty} e^{iux}\Big\{-\frac{\partial P_j}{\partial \tau} + \frac{1}{2}\nu\frac{\partial^2 P_j}{\partial x^2} - (\frac{1}{2} - j)\nu\frac{\partial P_j}{\partial x} + \frac{1}{2}\sigma^2\nu\frac{\partial^2 P_j}{\partial \nu^2} + \rho\sigma\nu\frac{\partial^2 P_j}{\partial x \partial v} + (a - b_j\nu)\frac{\partial P_j}{\partial \nu}\Big\}dx = 0 \tag{3.10}$$

Hence by using the Fourier transform as given in equation (3.29) and substituting this into equation (3.7) gives

$$-\frac{\partial \tilde{P}_j}{\partial \tau} - \frac{1}{2}u^2\nu\tilde{P}_j - (\frac{1}{2} - j)iu\nu\tilde{P}_j + \frac{1}{2}\sigma^2\nu\frac{\partial^2 \tilde{P}_j}{\partial \nu^2} + \rho\sigma iu\nu\frac{\partial \tilde{P}_j}{\partial v} + (a - b_j\nu)\frac{\partial \tilde{P}_j}{\partial \nu} = 0 \tag{3.11}$$

Then define

$$\alpha = -\frac{u}{2} - \frac{iu}{2} + iju \tag{3.12}$$

$$\beta = \kappa - j\rho\sigma - \rho\sigma iu \tag{3.13}$$

$$\gamma = \frac{\sigma^2}{2} \tag{3.14}$$

Then equation (3.11) becomes

$$\nu\left\{\alpha\tilde{P}_j - \beta\frac{\partial \tilde{P}_j}{\partial \nu} + \gamma\frac{\partial^2 \tilde{P}_j}{\partial \nu^2}\right\} + a\frac{\partial \tilde{P}_j}{\partial \nu} - \frac{\partial \tilde{P}_j}{\partial \tau} = 0 \tag{3.15}$$

Now substitute

$$\begin{aligned}\tilde{P}_j(u,\nu,\tau) &= \exp\{C(u,\tau)\theta + D(u,\tau)\nu\}\tilde{P}_j(u,\nu,0)\\ &= \frac{1}{iu}\exp\{C(u,\tau)\theta + D(u,\tau)\nu\} \qquad (3.16)\end{aligned}$$

To get $P_j(x,\nu,0)$ subject to the terminal conditions as $\tau \to 0$

$$\lim_{\tau\to 0} P_j(x,\nu,\tau) = \begin{cases} 1 & \text{if} \quad x > 0\\ 0 & \text{if} \quad x \leq 0\\ & = \quad \vartheta(x)\end{cases}$$

and given that Fourier transform of $P_j(x,\nu,\tau)$ can be written as $\tilde{P}_j(u,\nu,\tau) = \int_{-\infty}^{\infty} e^{iux}P_j(x,\nu,\tau)dx$ we get

$$\begin{aligned}\tilde{P}_j(u,\nu,0) &= \lim_{\tau\to 0}\int_{-\infty}^{\infty} e^{-iux}P_j(x,\nu,\tau)dx\\ &= \int_{-\infty}^{\infty} e^{-iux}P_j(x,\nu,0)dx\\ &= \int_{-\infty}^{\infty} e^{-iux}\vartheta dx\\ &= \frac{1}{iu} \qquad (3.17)\end{aligned}$$

It follows that

$$\frac{\partial \tilde{P}_j}{\partial \tau} = \left\{\theta\frac{\partial C}{\partial \tau} + \nu\frac{\partial D}{\partial \tau}\right\}\tilde{P}_j \tag{3.18}$$

$$\frac{\partial \tilde{P}_j}{\partial \nu} = D\tilde{P}_j \tag{3.19}$$

$$\frac{\partial^2 \tilde{P}_j}{\partial \nu^2} = D^2\tilde{P}_j \tag{3.20}$$

The equation (3.11) is satisfied if

$$\begin{aligned}\frac{\partial C}{\partial \tau} &= \kappa D \\ \frac{\partial D}{\partial \tau} &= \alpha - \beta D + \gamma D^2 \\ &= \gamma(D - r_+)(D - r_-) \end{aligned} \tag{3.21}$$

where we define

$$r_{\pm} = \frac{\beta \pm \sqrt{\beta^2 - 4\alpha\gamma}}{2\gamma} =: \frac{\beta \pm d}{\sigma^2} \tag{3.22}$$

Integrating equation (3.21) with terminal conditions $C(u, 0) = 0$ and $D(u, 0) = 0$ gives

$$D(u, \tau) = r_- \frac{1 - e^{-d\tau}}{1 - ge^{-d\tau}} \tag{3.23}$$

$$C(u, \tau) = \kappa \left\{ r_- \tau - \frac{2}{\sigma^2} \log \left( \frac{1 - ge^{-d\tau}}{1 - g} \right) \right\} \tag{3.24}$$

where we define

$$g := \frac{r_-}{r_+} \tag{3.25}$$

Taking the inverse transform using then the inverse transform is given by

$$P(x, \nu, \tau) = \int_{-\infty}^{\infty} \frac{1}{2\pi} e^{iux} \tilde{P}(u, \nu, \tau) du \tag{3.26}$$

and performing the complex integration gives the final form of the probabilities $P_j$ in the form of an integral of a real valued function.

$$P_j(x, \nu, T) = \frac{1}{2} + \frac{1}{\pi} \int_0^{\infty} Re \left( \frac{f_j(x, \nu, T)}{iu} \right) du \tag{3.27}$$

where

$$f_j(x, \nu, t) = \exp\{C_j(u, \tau)\theta + D_j(u, \tau)\nu + iux\} \tag{3.28}$$

To deduce the characteristic function from the option formula, we define the characteristic function by

$$\Phi_T(u) = \mathbb{E}[e^{iux_T} | x_t = 0]$$

and the probability of the final log-stock price $X_T$ being greater than the strike price is given by

$$\begin{aligned}\mathbb{P}(X_T > x) &= P_0(x, \nu, \tau) \\ &= \frac{1}{2} + \frac{1}{\pi} \int_0^{\infty} Re \left\{ \frac{\exp\{C_j(u, \tau)\theta + D_j(u, \tau)\nu + iux\}}{iu} \right\} du\end{aligned}$$

with $x = \ln(S_t/K)$ and $\tau = T - t$. Let the log-strike $y$ be defined by $y = \ln(K/S_t) = -x$. Then, the probability density function $p(y)$ is given by

$$\begin{aligned} p(y) &= -\frac{\partial P_0}{\partial y} \\ &= \frac{1}{2\pi}\int_{-\infty}^{\infty} \exp\{C(\bar{u},\tau)\theta + D(\bar{u},\tau)\nu - i\bar{u}y\}d\bar{u} \end{aligned}$$

Then

$$\begin{aligned} \Phi_T(u) &= \int_{-\infty}^{\infty} p(y)e^{iuy}dy \\ &= \frac{1}{2\pi}\int_{-\infty}^{\infty} \exp\{C(\bar{u},\tau)\theta + D(\bar{u},\tau)\nu\}d\bar{u}\int_{-\infty}^{\infty} e^{i(u-\bar{u})y}d\bar{u} \\ &= \int_{-\infty}^{\infty} \exp\{C(\bar{u},\tau)\theta + D(\bar{u},\tau)\nu\}d\bar{u}\delta(u-\bar{u}) \\ &= \exp\{C(u,\tau)\theta + D(u,\tau)\nu\} \end{aligned}$$

The formula is relatively easy to evaluate in Matlab. However, it is important to carefully evaluate the limits of the integral in $P_j$. This integral cannot be approximated exactly, but use of numerical integration techniques such as Gauss Lagendre or Gauss Lobatto integration can be utilized to obtain a reasonably accurate evaluation..

In a different expression of $C_j$ as is found in various literature (including Heston's), it turns out that the multi-valued logarithm in $C_j$ is usually restricted to the principle branch by setting $n = 0$ when implementing the Heston model. As a result, discontinuities occur each time the imaginary part of the argument of the logarithm crosses the negative real axis. This leads to wrong results when integrating $f_j$ as it is desirable to ensure that the integrands are continuous. However, as shown in Gatheral [21] consistent use of the principle logarithm leads to continuous integrands, and this form of the Heston model is recommended.

## 3.2 Fourier-Cosine Series Expansion (COS)

In the previous section we have shown that in the Fourier domain we can solve European contracts, as long as the characteristic function is known. Using the Fourier transform, we performed integration by means of quadrature rules. Fang and Oosterlee [15] propose the Fourier-cosine expansion (COS) as an alternative to quadrature integration techniques for methods based on Fourier transform. In their paper, they show that the COS method can improve the speed of pricing plain vanilla options. Although much focus is not placed on the COS method in this paper, we outline it here for completion. We apply the COS method to price European options under the Heston model and compare its results to those of call prices generated using the previously presented technique that uses quadrature integration. We have applied COS only to the Heston model to outline its viability, and have left the application to other models for future work. Details of the COS method can be found in the Fang and Oosterlee [15] paper.

### 3.2.1 Fourier-Cosine Expansion for Solving Inverse Fourier Integrals

Firstly, Fang and Oosterlee present a different methodology for solving the inverse Fourier integral in equation (2.16) by reconstructing the whole integral from its Fourier-cosine series expansion, extracting the series coefficients directly from the integrand. We follow this alternative technique here as presented in their 2008 paper [15].

For a function supported on $[0, \pi]$, the cosine expansion reads.

$$f(\theta) = {\sum_{k=0}^{\infty}}' A_k \cdot \cos(k\theta) \quad \text{with} \quad A_k = \frac{2}{\pi}\int_0^{\pi} f(\theta)\cos(k\theta)d\theta \tag{3.29}$$

where $\Sigma'$ indicates that the first term in the summation is weighted by a half. For functions on any other finite interval, say $[a, b] \in \mathbb{R}$, the Fourier-cosine series expansion can be obtained by a change of variables:

$$\theta := \frac{x-a}{b-a}\pi; \quad x = \frac{b-a}{\pi}\theta + a \tag{3.30}$$

It then reads

$$f(x) = {\sum_{k=0}^{\infty}}' A_k \cdot \cos(k\pi\frac{x-a}{b-a}) \tag{3.31}$$

with

$$A_k = \frac{2}{b-a}\int_a^b f(x)\cos\left(k\pi\frac{x-a}{b-a}\right)dx \tag{3.32}$$

The derivation starts with a truncation of the infinte integration range in (2.16), since any real function defined on a finite interval has a cosine expansion which converges under certain conditions. In this case, due to the existance of a Fourier transform, the integrands in (2.16) have to decay to zero at $\pm\infty$, and we can truncate the integration range in a proper way without losing accuracy.
Suppose $[a, b] \subset \mathbb{R}$ is chosen such that the truncated integral approximates the infinite counterpart very well, i.e.

$$\phi_1(\omega) := \int_a^b e^{i\omega x} f(x)dx \approx \int_{\mathbb{R}} e^{i\omega x} f(x)dx = \phi(w) \tag{3.33}$$

By using subscripts for variables like $i$ in $\phi_i$, we denote subsequent numerical approximations (not to be confused with subscripted series coefficients, $A_k$ and $F_k$). Comparing equation (3.33) with the cosine series coefficients of $f(x)$ on $[a, b]$ in (3.32), we find that

$$A_k = \frac{2}{b-a}\text{Re}\left\{\phi_1\left(\frac{k\pi}{b-a}\right) \cdot \exp\left(-i\frac{ka\pi}{b-a}\right)\right\} \tag{3.34}$$

where Re$\{\cdot\}$ denotes taking the real part of the argument. It then follows from (3.33) that $A_k \approx F_k$ with

$$F_k = \frac{2}{b-a}\text{Re}\left\{\phi\left(\frac{k\pi}{b-a}\right) \cdot \exp\left(-i\frac{ka\pi}{b-a}\right)\right\} \tag{3.35}$$

We now replace $A_k$ by $F_k$ in the series expansion of $f(x)$ on $[a, b]$, i.e.

$$f_1(x) = {\sum_{k=0}^{\infty}}' F_k \cos\left(k\pi\frac{x-a}{b-a}\right) \tag{3.36}$$

and truncate the series summation such that

$$f_2(x) = {\sum_{k=0}^{N-1}}' F_k \cos\left(k\pi\frac{x-a}{b-a}\right) \tag{3.37}$$

In their paper [15], Fang and Oosterlee show that we can expect (3.37) to give highly accurate approximations for small $N$.

### 3.2.2 Pricing Call Options

To price European options we use the risk-neutral valuation formula:

$$v(x,t_0) = e^{-r\Delta t}\mathbb{E}^{\mathbb{Q}}[v(y,T)|x] = e^{-r\Delta t}\int_{\mathbb{R}} v(y,T)f(y|x)dy \tag{3.38}$$

where $v$ denotes the option value, $\Delta t$ is the difference between the maturity $T$ and the initial date $t_0$, and $\mathbb{E}^{\mathbb{Q}}[\cdot]$ is the expectation operator under risk-neutral measure $\mathbb{Q}$. $x$ is a state variables at time $t_0$, while $f(y|x)$ is the probability density of $y$ given $x$. $r$ is the risk-neutral interest rate.

Since the density rapidly decays to zero as $y \to \pm\infty$ in (3.38), we truncate the infinite integration range without losing significant accuracy to $[a,b] \subset \mathbb{R}$, and we obtain approximation $v_1$

$$v_1(x,t_0) = e^{-r\Delta t}\int_a^b v(y,T)f(y|x)dy \tag{3.39}$$

Details on how to choose $[a,b]$ will be given below . In the next step, we replace the density function by its cosine expansion in $y$ since $f(y|x)$ is usually not known, whereas the characteristic function is.

$$f(y|x) = {\sum_{k=0}^{+\infty}}' A_k(x)\cos\left(k\pi\frac{y-a}{b-a}\right) \tag{3.40}$$

with

$$A_k(x) = \frac{2}{b-a}\int_a^b f(y|x)\cos\left(k\pi\frac{y-a}{b-a}\right)dy \tag{3.41}$$

so that

$$v_1(x,t_0) = e^{-r\Delta t}\int_a^b v(y,T){\sum_{k=0}^{+\infty}}' A_k(x)\cos\left(k\pi\frac{y-a}{b-a}\right)dy \tag{3.42}$$

We interchange the summation and integration, and insert the definition

$$V_k = \frac{2}{b-a}\int_a^b v(y,T)\cos\left(k\pi\frac{y-a}{b-a}\right)dy \tag{3.43}$$

resulting in

$$v_1(x,t_0) = \frac{1}{2}(b-a)e^{-r\Delta t}\cdot{\sum_{k=0}^{+\infty}}' A_k(x)V_k \tag{3.44}$$

We note that the $V_k$ are the cosine series coefficients of $v(y|t)$ in $y$. Hence, from (3.39) to (3.44) we have transformed the product of two real functions $f(y|x)$ and $v(y,T)$ to that of their Fourier-cosine series coefficients.

Due to the rapid decay rate of these coefficients, we can further truncate the series summation to obtain approximation $v_2$:

$$v_2(x, t_0) = \frac{1}{2}(b-a)e^{-r\Delta t} \cdot {\sum_{k=0}^{N-1}}' A_k(x) V_k \tag{3.45}$$

Similar to (3.35), $A_k(x)$ can be approximated by $F_k(x)$. Hence replacing this in (3.45), we obtain

$$v(x, t_0) \approx v_3(x, t_0) = e^{-r\Delta t} {\sum_{k=0}^{N-1}}' \mathrm{Re}\left\{\phi\left(\frac{k\pi}{b-a}; x\right) e^{-ik\pi \frac{a}{b-a}}\right\} V_k \tag{3.46}$$

which is the COS formula for general underlying processes.

To determine the interval of integration $[a, b]$ within the COS method, Fang and Oosterlee [15] propose the following:

$$[a, b] := \left[c_1 - L\sqrt{c_2 + \sqrt{c_4}}, c_1 + L\sqrt{c_2 + \sqrt{c_4}}\right] \quad \text{with} \quad L = 10 \tag{3.47}$$

Here, $c_n$ denotes the $n^{th}$ cumulant of $\ln(S_T/K)$. The cumulants $c_n$ are defined by the cumulant-generating function $g(t)$:

$$g(t) = \log E(e^{t\dot{X}}) \tag{3.48}$$

for some random variable $X$, and are given by the derivatives at zero of $g(t)$. The Heston model cumulants are presented in section (3.2.4) while those of other models are outlined extensively in the Fang and Oosterlee paper [15].

### 3.2.3 Coefficients $V_k$ for Plain Vanilla Options

To price with equation (3.46), we need to have the payoff coefficients $V_k$. Since we assume that the characteristic function of the log-asset price is known, we represent the payoff as a function of the log-asset price. We denote this log-asset price by

$$x := \ln(S_0/K) \quad y := \ln(S_T/K) \tag{3.49}$$

with $S_t$ the underlying price at time $t$ and $K$ being the strike price. The payoff for European options reads

$$v(y, T) \equiv [\alpha \cdot K(e^y - 1)]^+ \quad \text{with} \quad \alpha = \begin{cases} 1 & \text{for a call} \\ -1 & \text{for a put} \end{cases} \tag{3.50}$$

Before deriving $V_k$ from its definition in (3.43), we need the following two results. *The cosine series coefficients, $\chi_k$, of $g(y) = e^y$ on $[c, d] \subset [a, b]$* are

$$\chi_k(c,d) := \int_c^d e^y \cos\left(k\pi\frac{y-a}{b-a}\right)dy \tag{3.51}$$

*and the cosine series coefficients, $\psi_k$, of $g(y) = 1$ on $[c, d] \subset [a, b]$* are

$$\psi_k(c,d) := \int_c^d \cos\left(k\pi\frac{y-a}{b-a}\right)dy \tag{3.52}$$

*Proof.* By using calculus we can show that

$$\begin{aligned}\chi_k(c,d) \quad := \quad & \frac{1}{1+(\frac{k\pi}{b-a})^2}\Bigg[\cos\left(k\pi\frac{d-a}{b-a}\right)e^d - \cos\left(k\pi\frac{c-a}{b-a}\right)e^c \\ & + \frac{k\pi}{b-a}\sin\left(k\pi\frac{d-a}{b-a}\right)e^d - \frac{k\pi}{b-a}\sin\left(k\pi\frac{c-a}{b-a}\right)e^c\Bigg] \qquad (3.53)\end{aligned}$$

and

$$\psi_k(c,d) := \begin{cases} \left[\sin\left(k\pi\frac{d-a}{b-a}\right) - \sin\left(k\pi\frac{c-a}{b-a}\right)\right]\frac{b-a}{k\pi} & k \neq 0 \\ (d-c) & k = 0 \end{cases} \tag{3.54}$$

□

In the case of a call option, we obtain

$$\begin{aligned} V_k^{call} &= \frac{2}{b-a}\int_0^b K(e^y-1)\cos\left(k\pi\frac{y-a}{b-a}\right)dy \\ &= \frac{2}{b-a}K(\chi_k(0,b) - \psi(0,b)) \qquad (3.55)\end{aligned}$$

where $\chi_k$ and $\psi_k$ are given by (3.53) and (3.54) respectively. Similarly, for a vanilla put option, we find

$$V_k^{put} = \frac{2}{b-a}K(-\chi_k(0,b) + \psi(0,b)) \tag{3.56}$$

### 3.2.4 Application to the Heston Model

In the case of the Heston model, equation (3.35) can be simplified so that options for many strike prices can be computed simultaneously. We use boldfaced values to distinguish vectors.

In the Heston model, the characteristic function is represented by

$$\phi(\omega; \mathbf{x}, u_0) = \varphi_{hes}(\omega; u_0) \cdot e^{i\omega\mathbf{x}} \tag{3.57}$$

with $u_0$ being the volatility of the underlying at the initial time and $\varphi_{hes}(\omega; u_0) = \phi(\omega; 0, u_0)$. The pricing formula is simplified to

$$v(\mathbf{x}, t_0) \approx e^{-r\Delta t} {\sum_{k=0}^{N-1}}' \mathrm{Re}\left\{\varphi_{hes}\left(\frac{k\pi}{b-a}; u_0\right) e^{-ik\pi\frac{\mathbf{x}-a}{b-a}}\right\} \mathbf{V}_k \tag{3.58}$$

Recalling the $\mathbf{V}_k$ formulas for European call and put options in (3.55) and (3.56), we can now present them as a vector multiplied by a scalar,

$$\mathbf{V}_k = U_k \mathbf{K}$$

where

$$U_k = \begin{cases} \frac{2}{b-a}(\chi_k(0,b) - \psi(0,b)) & \text{for a call} \\ \frac{2}{b-a}(-\chi_k(0,b) + \psi(0,b)) & \text{for a put} \end{cases} \tag{3.59}$$

As a result, the pricing formula reads

$$v(\mathbf{x}, t_0, u_0) \approx \mathbf{K} e^{-r\Delta t} \cdot \mathrm{Re}\left\{ {\sum_{k=0}^{N-1}}' \varphi_{hes}\left(\frac{k\pi}{b-a}; u_0\right) U_k \cdot e^{-ik\pi\frac{\mathbf{x}-a}{b-a}} \right\} \tag{3.60}$$

where the summation can be written as a matrix-vector product if $\mathbf{K}$ is a vector, and $\varphi_{hes}(\omega; u_0)$ is the Heston characteristic function of the log-asset price.

Under the Heston model, Fang and Oosterlee [15] propose that instead of the formula given by equation (3.47), we define the truncation range instead by

$$[a, b] := \left[c_1 - L\sqrt{|c_2|}, c_1 + L\sqrt{|c_2|}\right] \quad \text{with} \quad L = 12. \tag{3.61}$$

Cumulant $c_2$ may become negative for sets of Heston parameters that do not satisfy the Feller condition, i.e., $2\kappa\theta > \sigma^2$. We therefore use the absolute value of $c_2$.

$c_1$ and $c_2$ are given by

$$c_1 = rT + (1 - e^{-\kappa T})\frac{\theta - v_0}{2\kappa} - \frac{1}{2}\theta T \tag{3.62}$$

$$\begin{aligned} c_2 = & \frac{1}{8\kappa^3}(\sigma T\kappa e^{-\kappa T}(v_0 - \theta)(8\kappa\rho - 4\sigma) \\ & +\kappa\rho\sigma(1 - e^{-\kappa T})(16\theta - 8v_0) \\ & +2\theta\kappa T(-4\kappa\rho\sigma + \sigma^2 + 4\kappa^2) \\ & +\sigma^2((\theta - 2v_0)e^{-2\kappa T} + \theta(6e^{-\kappa T} - 7) + 2v_0) \\ & +8\kappa^2(v_0 - \theta)(1 - e^{-\kappa T}) \end{aligned} \tag{3.63}$$

# 4 Adding Jumps

As has been discussed earlier, jumps have been observed to be important as they are needed to calibrate shorter maturities. In this chapter we derive the characteristic function of a jump diffusion model and a stochastic volatility jump diffusion model, which are used to generate volatility smiles in later chapters.

## 4.1 Jump Diffusion

The stock price dynamics of the stock price under jump diffusion are assumed to follow the SDE

$$dS = \mu S dt + \sigma S dW + (J-1) S dq \tag{4.1}$$

where $dW$ is a Brownian motion, $\sigma$ is the volatility of the geometric Brownian motion. $dq$ is the Poisson process independent of the Brownian motions with intensity $\lambda$ and

$$dq = \begin{cases} 0 & \text{with probability } 1-\lambda(t)dt \\ 1 & \text{with probability } \lambda(t)dt \end{cases}$$

$J$ is the relative jump size in the stock price. The jumps are independent and identically distributed with distribution $F$. Typical assumptions for the distribution of jump sizes are given below.

**Log-Normal Jump Diffusion**
Merton proposed jump diffusion where the logarithm of jump size is normally distributed.

$$F = \frac{1}{\sqrt{2\pi\delta^2}} e^{-\frac{(J-\nu)^2}{2\delta^2}}$$

As a result $e^J$ is log-normally distributed.

**Double-Exponential Jump Diffusion**
This model was introduced by S.G.Kou [22]. In this model the logarithm of the asset price is assumed to follow a Brownian motion plus a compound Poisson process with jump sizes double exponentially distributed.

$$F = p\frac{1}{\eta_u} e^{-\frac{1}{\eta_u}J} 1_{\{J\geq 0\}} + q\frac{1}{\eta_d} e^{\frac{1}{\eta_d}J} 1_{\{J<0\}}$$

where $1 > \eta_u > 0$, $\eta_d > 0$ are means of positive and negative jumps respectively; $p, q \geq 0$, $p+q=1$. $p$ and $q$ represent the probabilities of positive and negative jumps. The condition that $\eta_u < 1$ is to ensure that the stock price $S$ has a finite expectation.

### 4.1.1 Jump Diffusion PDE

In the case where the jump size $J$ is known, and following the same process as the Black Scholes model, the PDE for jump diffusion is given as

$$\frac{\partial V}{\partial t} + \frac{1}{2}\sigma^2 S^2 \frac{\partial^2 V}{\partial S^2} + rS\frac{\partial V}{\partial t} - rV + \lambda(S,t)\left\{V(JS,T) - V(S,t) - (J-1)S\frac{\partial V}{\partial S}\right\} = 0 \tag{4.2}$$

Typically we do not know in advance what the jump sizes are. A major draw-back of jump diffusion models with uncertain jump sizes is that there is no replicating portfolio. Hence to extend equation (4.2) to the case of unknown jump sizes, we assume that the risk-neutral process is still a jump diffusion with jumps independent of the stock price. Under the risk-neutral measure, the expected return of any asset is the risk-free rate. Hence taking expectations of the SDE given in equation (4.1), we find that

$$\mathbb{E}[dS/S] = rdt = \mu dt + \mathbb{E}[J-1]\lambda(t)dt \tag{4.3}$$

It follows that the risk-neutral drift is given by $\mu = r + \mu_j$ with

$$\mu_j = -\lambda(t)\mathbb{E}[J-1]$$

Similar to the derivation of the Black Scholes equation, applying Itô's lemma and taking expectations under the risk-neutral measure, the European-style option satisfies the following PDE. Complete derivation can be found in [21].

$$\frac{\partial V}{\partial t} + rS\frac{\partial V}{\partial S} + \frac{1}{2}\sigma^2 S^2 \frac{\partial^2 V}{\partial S^2} - rV + \lambda(t)\left\{\mathbb{E}[V(JS,t) - V(S)] - \mathbb{E}[J-1]S\frac{\partial V}{\partial S}\right\} = 0 \tag{4.4}$$

## 4.2 Pricing by Fourier Transform

Given a characteristic function, European call options can be priced using Fourier methods as in Lewis [1].

### 4.2.1 Characteristic Function for Jump Diffusion Model

We follow closely the derivation of the characteristic function as given in Gatheral [21]. With a constant intensity rate $\lambda$, the logarithmic version of the jump diffusion process for the underlying asset is an example of a Lêvy process.

Definition: *A Lêvy process is a continuous in probability, cádlág stochastic process $x(t) > 0$ with independent and stationary increments and $x(0) = 0$.*

As depicted in Lewis[1], Lêvy processes can be expressed as the sum of a linear drift term, a Brownian motion, and a jump process. This plus the independent increment property leads directly to the following representation of the characteristic function.

**The Lêvy-Khintchine representation**
If $x_t$ is a Lêvy process, and if the Lêvy density $\mu(\chi)$ is suitably well behaved at the origin, its characteristic function $\phi_T(u) := \mathrm{E}[e^{iu\chi_T}]$ has the representation

$$\phi_T(u) = exp\bigg\{iu\omega T - \frac{1}{2}u^2\sigma^2 T + T\int[e^{iu\chi} - 1]\mu(\chi)d\chi\bigg\} \tag{4.5}$$

To get the drift parameter $\omega$, we impose that the risk-neutral expectation of the stock price be the forward price and we assume zero interest rates and dividends. This translates to

$$\phi_T(-i) = \mathrm{E}[e^{x_T}] = 1$$

$\int \mu(\chi)d\chi = \lambda$, the Poisson intensity or mean jump arrival rate.

In Merton's model the jump-size $J$ is assumed to be log-normally distributed with mean log-jump $\alpha$ and standard deviation $\delta$ so that the stock price follows the SDE

$$dS = \mu S dt + \sigma S dW + (e^{\alpha+\delta\varepsilon} - 1)S dq \tag{4.6}$$

with $\varepsilon \sim N(0,1)$. Then

$$\mu(\chi) = \frac{\lambda}{\sqrt{(2\pi\delta^2)}}\exp\bigg\{ - \frac{(\chi-\alpha)^2}{2\delta^2}\bigg\}$$

By applying the Lêvy-Khintchine representation to equation (4.5), we see that the characteristic function is given by

$$\begin{aligned}\phi_T(u) &= \exp\bigg\{iu\omega T - \frac{1}{2}u^2\sigma^2 T + T\int\bigg[e^{iu\chi} - 1\bigg]\frac{\lambda}{\sqrt{2\pi\delta^2}} \\ &\qquad \exp\bigg\{ - \frac{(\chi-\alpha)^2}{2\delta^2}\bigg\}d\chi\bigg\} \\ &= \exp\bigg\{iu\omega T - \frac{1}{2}u^2\sigma^2 T + \lambda T\Big(e^{iu\alpha - u^2\delta^2/2} - 1\Big)\bigg\} \end{aligned} \tag{4.7}$$

To get $\omega$, we impose $\phi_T(-i) = 1$ so that

$$\exp\left\{\omega T + \frac{1}{2}\sigma^2 T + \lambda T(e^{\alpha+\delta^2} - 1)\right\} = 1$$

which gives

$$\omega = -\frac{1}{2}\sigma^2 - \lambda(e^{\alpha+\delta^2/2} - 1)$$

If we set $\alpha = \delta = 0$ we get the log-normal case.

Alternatively we can get the characteristic function for jump diffusion directly by substituting $\phi_T(u) = e^{\psi(u)T}$ into equation (4.7). With $y \sim N(\alpha, \delta)$ we get

$$\begin{aligned}
\psi(u) &= -\frac{1}{2}u(u+i)\sigma^2 - \lambda\left\{\mathbb{E}[e^{iuy} - 1] + iu\mathbb{E}[e^y - 1]\right\} \\
&= -\frac{1}{2}u(u+i)\sigma^2 - \lambda\left\{\left(e^{iu\alpha - u^2\delta^2/2} - 1\right) + iu\left(e^{\alpha+\delta^2/2} - 1\right)\right\} \quad (4.8)
\end{aligned}$$

This gives an expression for $\phi_T(u)$ similar to the one derived in equation (4.6).

### 4.2.2 Option Pricing

Carr and Madan [6] and Lewis [1] show that it is quite straightforward to get option prices by inverting the characteristic function of a given stochastic process if it is known in closed form.

We follow the proof given by Gatheral [21] to compute the option pricing formula from the characteristic function. The call option formula $C(S, K, T)$ is a special case of formula (2.10) given by Lewis [1]. We assume zero interest rates and zero dividends

$$C(S, K, T) = S - \sqrt{SK}\frac{1}{\pi}\int_0^\infty \frac{du}{u^2 + \frac{1}{4}}\mathrm{Re}[e^{iuk}\phi_T(u - i/2)] \quad (4.9)$$

with $k := \log(K/S)$.

**Proof**

A covered call option has the payoff $\min[S_T, K]$ where $S_T$ is the stock price at time $T$ and $K$ is the strike price of the call. Consider the Fourier transform of this covered call position $G(k,\tau)$ with respect to the log-strike $k := \log(K/S)$ defined by

$$\hat{G}(u,\tau) = \int_{-\infty}^{\infty} e^{iuk} G(k,\tau)dk$$

Denoting the current time by $t$ and expiration by $T$, we have

$$\begin{aligned}
\hat{G}(u, T-t) &= \int_{-\infty}^{\infty} e^{iuk}\mathbb{E}\Big[\min(e^{x_T}, e^k)^+ | x_t = 0\Big] dk \\
&= \mathbb{E}\Big[\int_{-\infty}^{\infty} e^{iuk}[\min(e^{x_T}, e^k)^+ dk] | x_t = 0\Big] \\
&= \mathbb{E}\Big[\int_{-\infty}^{x_T} e^{iuk} e^k dk + \int_{x_T}^{\infty} e^{iuk} e^{x_T} dk] | x_t = 0\Big] \\
&= \mathbb{E}\Big[\frac{e^{(1+iu)x_T}}{1+iu} - \frac{e^{(1+iu)x_T}}{iu}\Big| x_t = 0\Big] \text{only if} \quad 0 < \mathrm{Im}[u] < 1 \\
&= \frac{1}{u(u-i)}\mathbb{E}\Big[e^{(1+iu)x_T}\Big| x_t = 0\Big] \\
&= \frac{1}{u(u-i)}\phi_T(u-i) \qquad (4.10)
\end{aligned}$$

by definition of the characteristic function $\phi_T(u)$. Note that the transform of the covered call value exists only if $0 < \mathrm{Im(u)} < 1$. The derivation would work for other payoffs, though it is important to note that the region where the transform exists depends on the payoff.
To get the call price in terms of the characteristic function, we express it in terms of the covered call and invert the Fourier transform, integrating along the line Im(u)=1/2 [21]. Then

$$\begin{aligned}
C(S,K,T) &= S - S\frac{1}{2\pi}\int_{-\infty+i/2}^{\infty+1/2} \frac{du}{u(u-i)}\phi_T(u-i)e^{-iku} \\
&= S - S\frac{1}{2\pi}\int_{-\infty}^{\infty} \frac{du}{(u+i/2)(u-i/2)}\phi_T(u-i/2)e^{-ik(u-i/2)} \\
&= S - \sqrt{SK}\frac{1}{\pi}\int_0^{\infty} \frac{du}{(u^2+\frac{1}{4})}\mathrm{Re}\big[e^{-iuk}\phi_T(u-i/2)\big] \qquad (4.11)
\end{aligned}$$

with $k = \log(K/S)$.

## 4.3 Stochastic Volatility Plus Jumps

As has been discussed it is natural to combine stock price jumps and stochastic volatility in one model.

If we add a log-normally distributed jump process to the Heston process as suggested in the Merton model, the stock price and variance satisfy the following SDE

$$dS = \mu S dt + \sqrt{\nu} S dW_1 + (e^{\alpha+\delta\epsilon} - 1) S dq \tag{4.12}$$

$$d\nu = \kappa(\theta - \nu)dt + \sigma_v \sqrt{\nu} dW_2 \tag{4.13}$$

with $\langle dW1, dW_2 \rangle = \rho dt, \epsilon \sim N(0,1)$ and as in the jump diffusion case, the Poisson process

$$dq = \begin{cases} 0 \text{ with probability } 1 - \lambda_J dt \\ 1 \text{ with probability } \lambda_J dt \end{cases}$$

where $\lambda_J$ is the jump intensity. Since the jump part and the diffusion part are independent, the characteristic function would be the product of Heston and jump diffusion characteristic functions. Specifically,

$$\phi_T(u) = e^{C(u,T)\theta + D(u,T)V_t} e^{\psi(u)T}$$

with

$$\psi(u) = -\lambda_J iu(e^{\alpha+\delta^2/2} - 1) + \lambda_J(e^{iu\alpha - u^2\delta^2/2} - 1)$$

and $C(u,T), D(u,T)$ are as expressed in chapter 3.

### 4.3.1 Other Stochastic and Volatility Models

Other models that are modifications of the stochastic volatility and jump models are summarized in this section. Because this is not the focus of this paper, we only give the SDE's, followed by the models and a brief commentary.

**Jump Diffusion with Stochastic Volatility and Jump Intensity**
Fang [14] looked at Bates model [3] with a stochastic jump intensity rate

$$\begin{aligned} dS(t) &= (r - d - \lambda m)S(t)dt + \sqrt{V(t)}S(t)dW^s(t) + (e^J - 1)S(t)dN(t), S(0) = S; \\ dV(t) &= \kappa(\theta - V(t))dt + \epsilon\sqrt{V(t)}dW^\nu(t), V(0) = V; \\ d\lambda(t) &= \kappa_\lambda(\theta_\lambda - \lambda(t))dt + \epsilon_\lambda\sqrt{\lambda(t)}dW^\lambda(t), \lambda(0) = \lambda. \end{aligned}$$

where $\kappa_\lambda$ is a mean-reverting rate, $\theta_\lambda$ is a long term intensity, $\epsilon_\lambda$ is the volatility of jump intensity, a Weiner process $W^\lambda(t)$ is independent of $W^x(t)$ and $W^\nu(t)$ [2].

**Jump Diffusion with Deterministic Volatility and Jump Intensity**
In this model the following dynamics are assumed.

$$
\begin{aligned}
dS(t) &= (r - d - \lambda m)S(t)dt + \sqrt{V(t)}S(t)dW^s(t) + (e^J - 1)S(t)dN(t), S(0) = S; \\
dV(t) &= \kappa(\theta - V(t))dt, V(0) = V; \\
d\lambda(t) &= \kappa_\lambda(\theta_\lambda - \lambda(t))dt, \lambda(0) = \lambda.
\end{aligned}
$$

A similar model, but in discrete GARCH specification, was considered in the empirical studies by Maheu and McCurdy [24]. They found that the model provides a good fit for data, and is capable of producing a variety of implied distributions [2].

**Jump Diffusion with Price and Volatility Jumps**
Duffie-Pan-Singleton [12] proposed a jump diffusion with both price and volatility jumps (SVJ)

$$
\begin{aligned}
S(t) &= (r - d - \lambda m)S(t)dt + \sqrt{V(t)}S(t)dW^s(t) + (e^{J^s} - 1)S(t)dN^s(t), S(0) = S; \\
dV(t) &= \kappa(\theta - V(t))dt + \epsilon\sqrt{V(t)}dW^\nu(t) + J^\nu dN^\nu(t), V(0) = V;
\end{aligned}
$$

This model looks at four types of jumps

- Jumps in the asset price
- Jumps in the variance with exponential distributed jump size
- Double jumps model with jumps in the asset price and independent jumps in the variance with exponentially distributed jump size
- Simultaneous jumps model (SVSJ) with simultaneous correlated jumps in price and variance

This model is supported by studies done by Eraker-Johannes-Polson [13] and they found it provides a remarkable fit to observed volatility surfaces [2].

# 5 Barrier Options

A barrier option is a path-dependent option whose payoff at maturity depends on whether or not the underlying spot price has touched a pre-defined barrier during the life of the option. Barrier options trade over the counter, and are attractive because they are less expensive than the regular options. There are mainly two types of barrier options, namely *knock-out options* and *knock-in options*. A knock-out option ceases to exist when the underlying asset price reaches a certain barrier, while a knock-in option comes into existence when the underlying asset price reaches a pre-defined barrier.

In this thesis we will limit our attention to four barrier options,namely down-and-in, down-and-out, up-and-in and up-and-out call options. The first two are are examples of knock-out options, while the latter pair are examples of knock-in options.

To describe the payoff structure of the barrier option, we define the minimum and maximum and of the spot price process $P = \{S_t, 0 < t < T\}$ as $I_P = \inf\{S_t; 0 < t, T\}$ and $S_P = \sup\{S_t; 0 < t, T\}$

The down-and-out barrier is a normal European call option with strike K unless the underlying spot price hits a pre-determined barrier H, $H < S$ during the life of the option, in which case it becomes worthless. Its payoff at maturity is given by:

$$DOB = e^{-rT} E_Q[(S_T - K)^+ 1(S_P > H)] \tag{5.1}$$

where $1(S_P > H)$ is an indicator function equal to one if $S_P > H$ and zero otherwise.

The down-and-in barrier call is worthless unless the underlying spot price $S$ hits a pre-determined barrier H, $H < S$, during the life of the option in which case it becomes a plain vanilla call option with strike K. If this barrier is never reached during the life-time of the option, the option remains worthless. Its payoff at maturity is given by:

$$DIB = e^{-rT} E_Q[(S_T - K)^+ 1(I_P \leq H)] \tag{5.2}$$

The up-and-out barrier is a standard call option unless the underlying spot price hits a pre-determined barrier H, $H > S$, in which case it becomes worthless. Its payoff at maturity is given by:

$$UOB = e^{-rT} E_Q[(S_T - K)^+ 1(I_P < H)] \tag{5.3}$$

The up-and-in barrier is worthless unless the underlying spot price hits a pre-determined barrier H, $H > S$, in which case becomes a plain vanilla call option with strike K. Its payoff at maturity is given by:

$$UIB = e^{-rT} E_Q[(S_T - K)^+ 1(S_P \geq H)] \tag{5.4}$$

To price the path-dependent barrier options using the stochastic volatility, we use Monte Carlo simulation by reformulating the continuous process of the various models to discrete time.

# 6 The Calibration Problem

The previous chapter gives details on how to derive formulas to calculate call options for a given set of parameters that characterize the jump and volatility components. However, in reality, estimating the parameters to use in the model is just as important as the model itself. The Heston model has six parameters that need estimation; $\kappa, \theta, \sigma, V_0, \rho, \lambda$. The jump diffusion model has three, namely; $\mu, \delta, \lambda$. There are two ways to estimate these parameters: One can either use historical data to estimate parameters of the stock process or use market prices of liquid options to imply these parameters from option prices [2]. Studies relating to parameter estimation using historical time series are covered by Bates [3], Duffie-Pan-Singleton [11].

In this paper, we consider parameter estimation using an implied volatility matrix which takes into account information of liquid options across all possible strikes and maturities. Table 2 depicts a volatility matrix which contains the DAX (The Deutscher Aktienindex) option implied volatilities of March 3rd 2008 from Reuters [25]. As such, the most common way to solve the calibration problem is to minimize the error or discrepancy between model volatilities and observed market volatilities. This turns out to be a non-linear least squares optimization problem. More specifically the squared difference between the vanilla option volatilities and that of the model is minimized over the specific parameters as depicted below.

$$\min_{\Theta} \sum_{j-1}^{N} = \frac{1}{w_j} (\sigma_j^{\text{market}}(K,T) - \sigma_j^{\text{model}}(K,T;\Theta))^2 \tag{6.1}$$

where $\sigma_j^{\text{market}}$(K,T) is the market implied volatility for strike $K$ and maturity $T$, and $\sigma_j^{\text{model}}(K,T;\Theta)$ is the Black Scholes volatility, implied from the model price of a call option with strike $K$ and maturity $T$. $\omega_j$ is an appropriately chosen weight.

## 6.1 Calibration Method

The pricing model was coded in Matlab, and as such we used Matlab's least squares non linear optimizer *lsqnonlin*$(fun, x_0, lb, ub)$. The function minimizes the vector valued function, $fun$, using the vector of initial parameter values, $x_0$, where the lower and upper bounds of the parameters are specified in vectors $lb$ and $ub$, respectively.

The result produced by *lsqnonlin* is determined by the initial estimate of $x_0$. However, as long as the minimization equation is satisfied, the solution is acceptable, otherwise the process is rerun with a different $x_0$.

Apart from the obvious bounds on the parameters, such as non-negative speed of mean-reversion and variances, we also implemented the Feller conditions, namely that $2\kappa\theta < \sigma^2$. The Feller condition ensures that the variance process is strictly positive and cannot reach zero. This condition is implemented by introducing a variable $\psi = 2\kappa\theta - \sigma^2$. This variable is then used for optimization instead of the variable $\kappa$. The Feller condition then reduces to $\psi > 0$, and $\kappa$ can then be calculated as $\kappa = (\psi + \sigma^2)/2\theta$. This works in theory, however, the discretized version can still have negative paths, and this still needs to be checked.

The weighting $\omega_j$ is chosen such that all maturities are given the same weight in the calibration. Within each maturity category, all options are assigned equal weights. This is defined as:

$$\omega_j = \frac{1}{n_m \cdot n_{k_m}} \tag{6.2}$$

where $n_m$ is the number of maturities and $n_{k_m}$ is the number of options with the same maturity as option $j$. This choice of weighing is also used in [27].

## 6.2 Calibration Parameters of the Merton Model, SV Heston Model and SVJ Bates Model

DAX (The Deutscher Aktienindex) option implied volatilities of 3rd March 2008 are used for the calibration process. The data can be seen in Table 2.

The results of the estimated parameters are as follows:

Table 1:

| Estimated Parameters | | | |
|---|---|---|---|
| Parameter | MJD Estimates | SV Estimates | JD-SV Estimates |
| $\rho$ | | -0.9535 | -0.7916 |
| $\theta$ | | 0.0936 | 0.1049 |
| $\kappa$ | | 2.1689 | 3.4412 |
| $\sigma_v$ | | 0.3309 | 0.4529 |
| $V_0$ | | 0.1123 | 0.0889 |
| $\lambda$ | 0.4706 | | 0.0837 |
| $\mu$ | -0.2586 | | 0.0779 |
| $\delta$ | 0.4293 | | 0.0720 |

$V_0$ is spot variance; $\kappa$ is mean reversion speed; $\theta$ is long term variance; $\sigma_v$ is volatility of volatility; $\rho$ is correlation between price and variance.

$\lambda, \mu, \delta$ are jump intensity, mean and volatility for the Merton jump diffusion respectively.

**Jump diffusion** parameters show a negative mean and the jump intensity is small at 0.4706.

**Stochastic Volatility** parameters depict a negative correlation $\rho$ between the asset price and volatility, which is not uncommon in equity markets. The mean reversion $\kappa$ is relatively high at 2.1689.

**Jump diffusion with stochastic volatility**. Combining stochastic volatility and jump models produces better results than either one alone as depicted in figure 5. Introducing jumps improves the overall quality of calibration and handles the short maturities better. This can be observed in bar graph showing difference in implied volatility between the market and the model, where values between zero and one year have been reduced significantly from those of the SV model. The remaining values from one year and above remain relatively the same. The calibrated parameters show a small increase in $\sigma_v$ values and mean reversion $\kappa$ compared to the Heston model.

## 6.3 Quality of Calibration for Selected Models

Table 2 gives the implied volatility matrix of DAX options of 3rd March 2008 used in model calibration. The spot price is $S = 6689.95$. DAX options are European type options, with a risk free rate that is constant at 3% and no dividend yield applies.

Table2: Dax Implied Volatility Data

| Time | 2wks | 1.5m | 2.5m | 3m | 6m | 9m | 15m | 21m | 27m |
|---|---|---|---|---|---|---|---|---|---|
| Expiry | Mar-08 | Apr-08 | May-08 | Jun-08 | Sept-08 | Dec-08 | Jun-09 | Dec-09 | Jun-10 |
| Date | 20th | 18th | 16th | 20th | 19th | 19th | 19th | 18th | 18th |
| T | 0.0472 | 0.1278 | 0.2056 | 0.3028 | 0.5556 | 0.8083 | 1.3139 | 1.8194 | 2.3250 |
| Strike | | | | | | | | | |
| 5000 | 0.5158 | 0.5081 | 0.4801 | 0.4638 | 0.4300 | 0.4176 | 0.4096 | 0.4159 | 0.4252 |
| 5200 | 0.4839 | 0.4713 | 0.4505 | 0.4387 | 0.4095 | 0.3991 | 0.3933 | 0.4007 | 0.4104 |
| 5400 | 0.4553 | 0.4395 | 0.4250 | 0.4160 | 0.3906 | 0.3820 | 0.3780 | 0.3864 | 0.3966 |
| 5600 | 0.4324 | 0.4124 | 0.4019 | 0.3949 | 0.3728 | 0.3660 | 0.3636 | 0.3730 | 0.3837 |
| 5800 | 0.4094 | 0.3886 | | 0.3752 | 0.3559 | 0.3508 | 0.3500 | 0.3605 | 0.3716 |
| 6000 | 0.3866 | 0.3666 | 0.3606 | 0.3559 | 0.3396 | 0.3364 | 0.3371 | 0.3486 | 0.3601 |
| 6200 | 0.3636 | 0.3451 | 0.3406 | 0.3368 | 0.3239 | 0.3224 | 0.3248 | 0.3371 | |
| 6400 | 0.3401 | 0.3234 | 0.3203 | 0.3180 | 0.3085 | 0.3089 | 0.3130 | 0.3261 | 0.3389 |
| 6600 | 0.3155 | 0.3012 | 0.2998 | 0.2994 | 0.2937 | 0.2959 | 0.3017 | 0.3157 | 0.3290 |
| 6800 | 0.2901 | 0.2788 | 0.2797 | 0.2813 | 0.2796 | 0.2833 | 0.2908 | 0.3057 | 0.3196 |
| 7000 | 0.2663 | 0.2581 | 0.2608 | 0.2641 | | 0.2713 | 0.2804 | 0.2962 | 0.3105 |
| 7200 | 0.2519 | 0.2403 | 0.2440 | 0.2483 | 0.2540 | 0.2599 | 0.2705 | 0.2871 | 0.3018 |
| 7400 | 0.2466 | 0.2258 | 0.2293 | 0.2344 | 0.2425 | 0.2491 | 0.2612 | 0.2785 | 0.2934 |
| 7600 | 0.2473 | 0.2154 | 0.2171 | 0.2227 | 0.2313 | 0.2391 | 0.2523 | 0.2703 | 0.2854 |
| 7800 | 0.2604 | 0.2099 | 0.2075 | 0.2132 | | 0.2299 | 0.2442 | 0.2628 | 0.2780 |
| 8000 | 0.2799 | 0.2103 | 0.2017 | 0.2055 | 0.2119 | 0.2218 | 0.2366 | 0.2556 | 0.2711 |

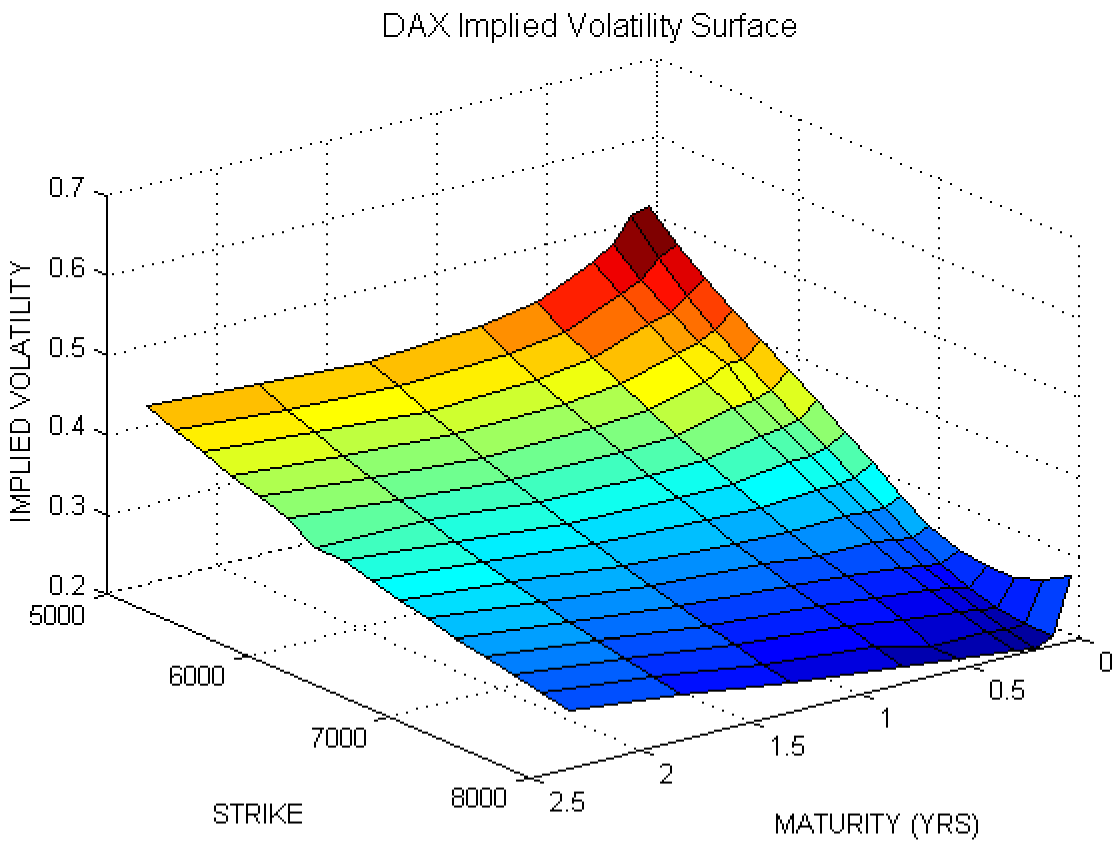


Figure 1: Dax implied volatility surface of March 2008

**Stochastic Volatility**

From the two figures below, the Heston model appears to match the middle term and long term maturities relatively well.

Figure 2: Model implied volatility surface

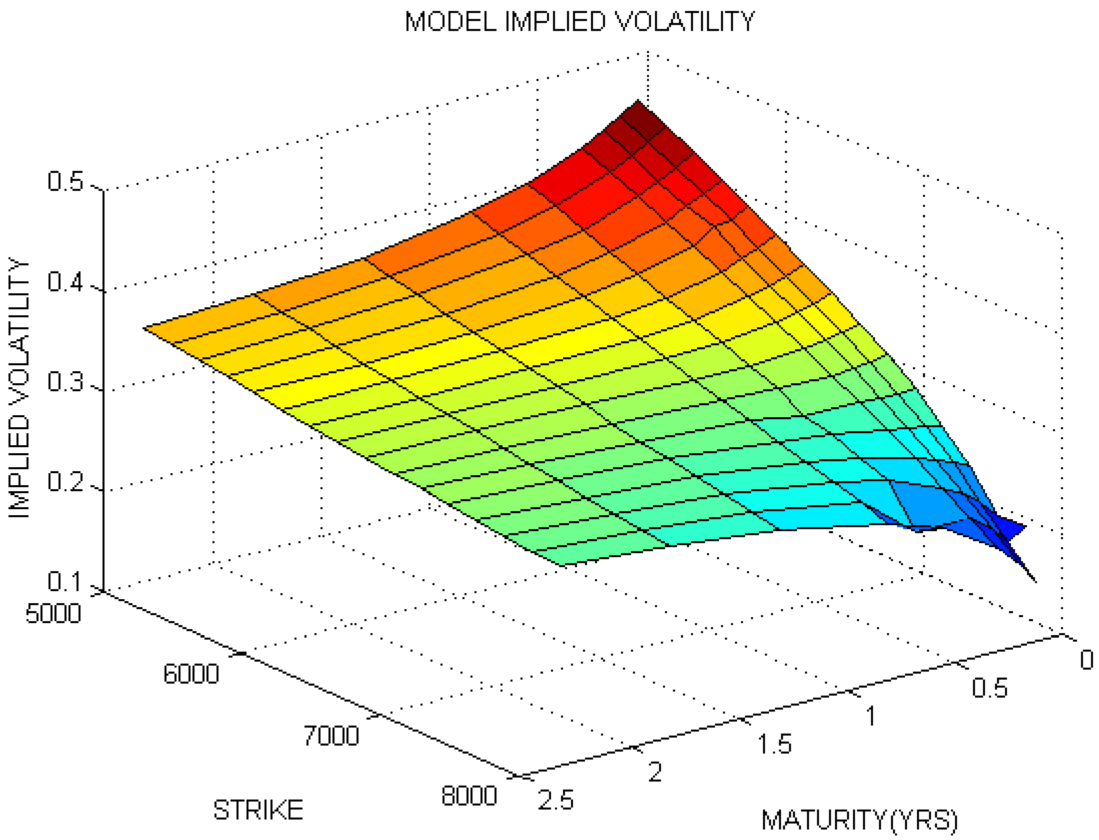

Figure 3: Difference in implied volatility

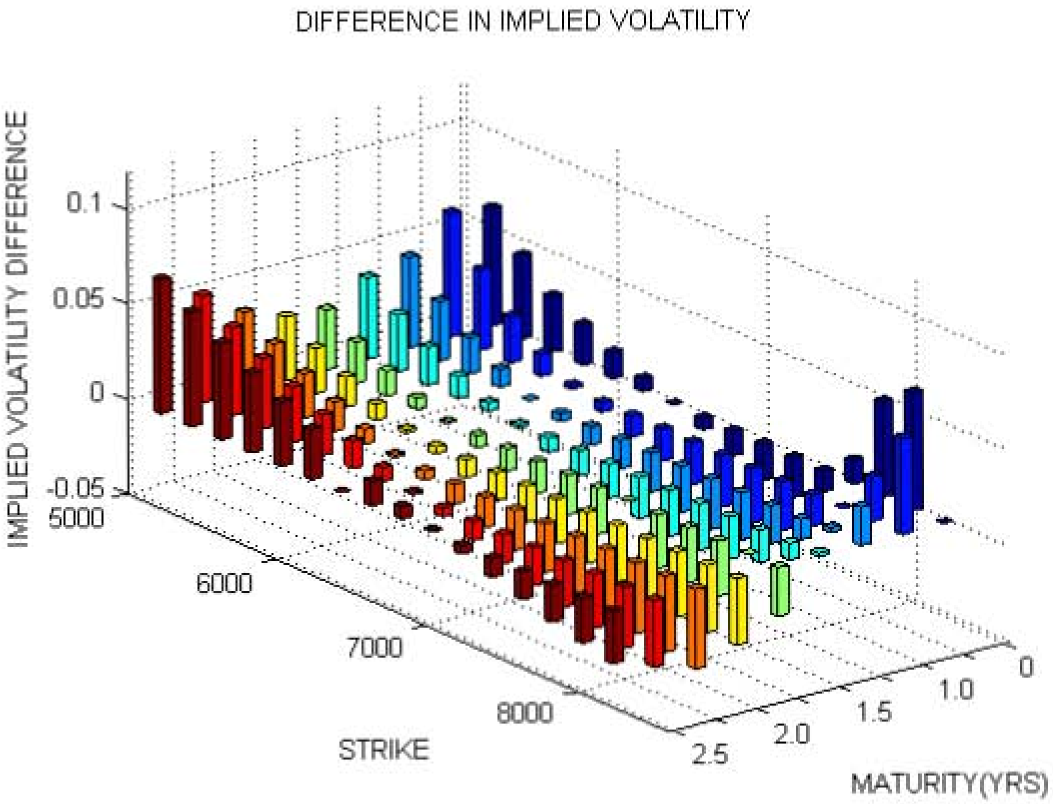

**Log Normal Jump Diffusion with Stochastic Volatility**
Combining both jump diffusion and stochastic volatility as per the Bates model leads to a better fit across all maturities. The bar graph shows the difference in volatility for shorter maturities (below one year) is reduced significantly across all strikes. For maturities above one year there does not seem to be a significant change compared to the values in the stochastic volatility model.

Figure 4: Model implied volatility

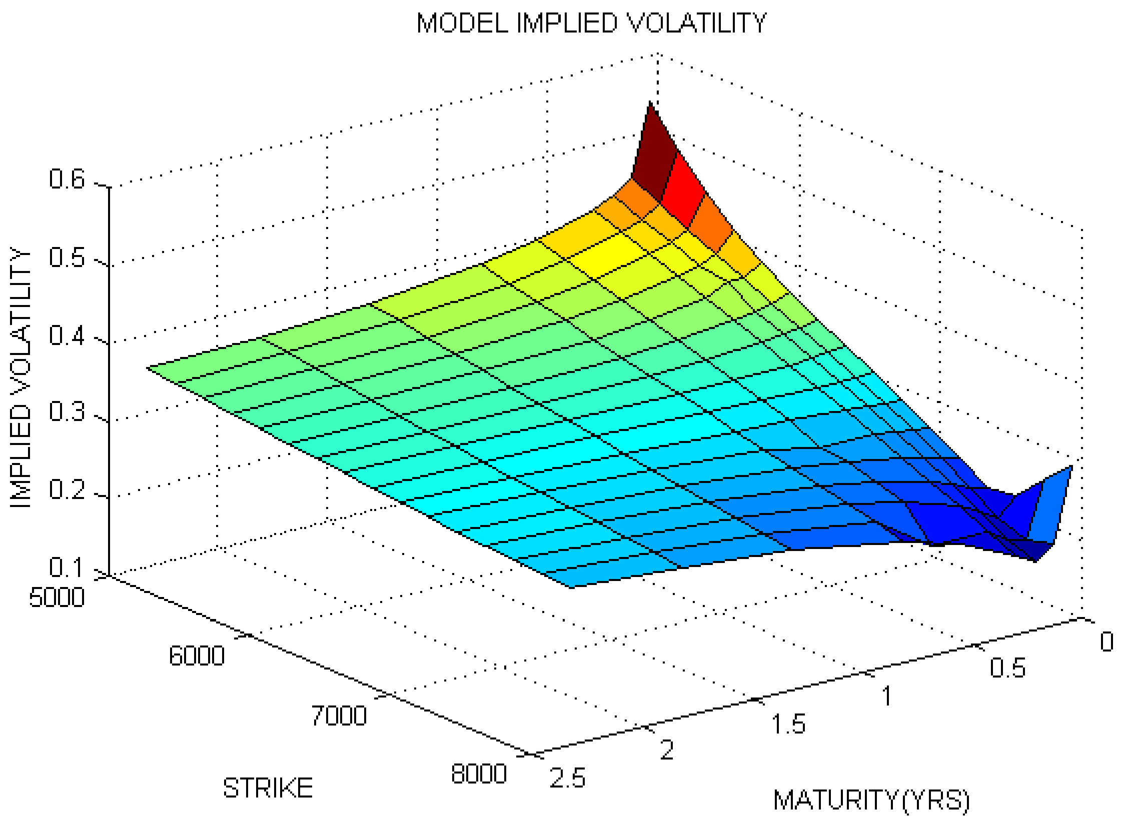

Figure 5: Difference in implied volatility

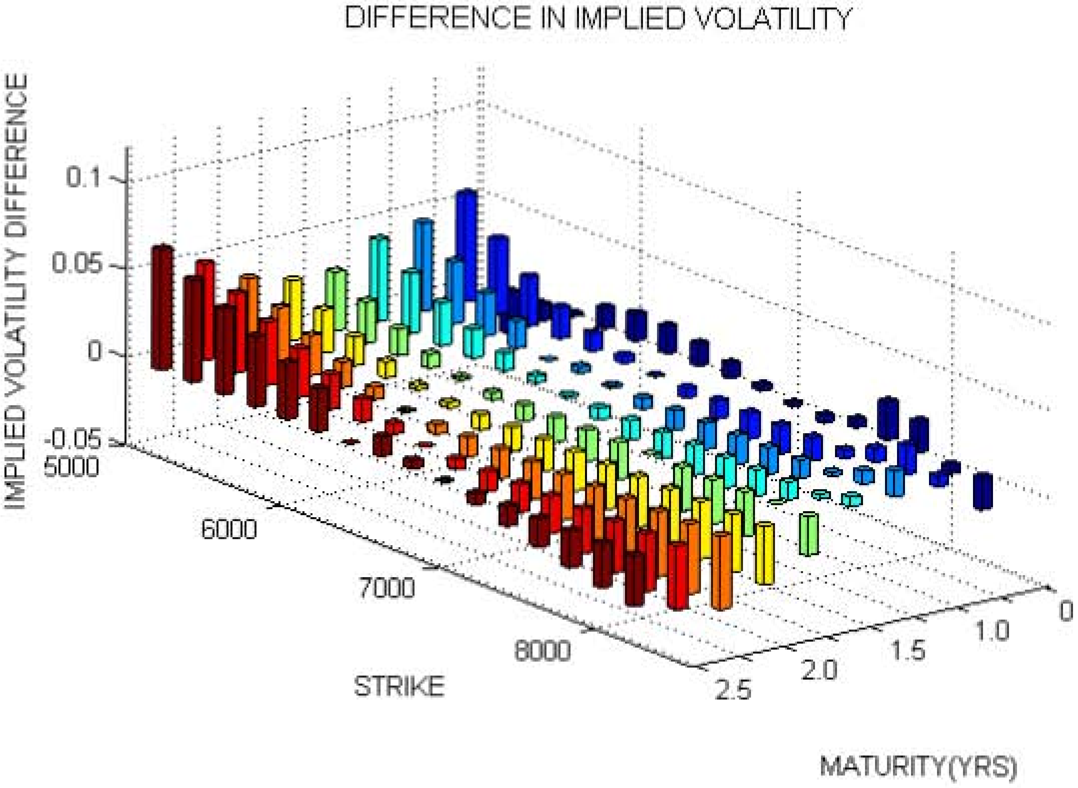

# 7 Implementation and Numerical Results

This section contains the various ways that one can implement the models introduced in the previous chapters. Focus is given to the Fourier transform method, exact simulation by Broadie and Kaya [5] and Monte Carlo methods.

## 7.1 Pricing via Fourier Transform

The closed-form European call option solution as given in chapter 3 is relatively straightforward to implement. The main challenge lies in computing the Fourier integral.

$$P_j(x, \nu_t, T, K) = \frac{1}{2} + \frac{1}{\pi} \int_0^\infty Re\left\{ \frac{\exp\{C_j(u,\tau)\theta + D_j(u,\tau)\nu + iux\}}{iu} \right\} du$$

The integral cannot be evaluated exactly but can be approximated with reasonable accuracy by some numerical integration techniques. We use Gaussian quadrature for this evaluation.

In Matlab, this can be done using two functions, quad(@$fun, a, b$) and quadl(@$fun, a, b$). However, the argument $b$ cannot be specified as infinity as the function quad(@$fun, a, b$) evaluates only proper integrals. Gatheral covers this in detail in his book "The Volatility surface" and shows the integrand converges very quickly to zero [21]. Hence for our purposes the limit of $b = 100$ is considered adequate.

The same processes has been used to implement the Bates model, using quadl(@$fun, a, b$) to compute the integral. Remembering that the characteristic function $f_j(x, \nu_t, T, \phi)$ is given by

$$e^{C(u,T)\theta + D(u,T)V_t} e^{\psi(u)T}$$

with

$$\psi(u) = -\lambda_J iu(e^{\alpha+\delta^2/2} - 1) + \lambda_J(e^{iu\alpha - u^2\delta^2/2} - 1)$$

Under the COS method, given that the formulas for the Heston cumulants are available from the Fang and Oosterlee Paper [15], it is relatively straightforward to implement this method in matlab.

## 7.2 Monte Carlo Simulation

Recall the Heston process

$$dS_t = \mu S_t dt + \sqrt{V_t} S_t dW_1$$

$$dV_t = \kappa(\theta - V_t)dt + \sigma_v \sqrt{V_t} dW_2$$

with

$$(dW_1, dW_2) = \rho dt$$

The Euler discretization method can be used to approximate the paths of the stock price and variance processes on a discrete time grid. The time grid is divided into M equal sections of length $\Delta t$, that is, $t_i = iT/M$ for each $i = 0, 1, ..., M$. The discretization of the stock process is in the form of $x_i = \log(S_i/S_0)$

$$x_{t_i} = x_{t_{i-1}} + (r - \frac{V_{t_{i-1}}}{2})\Delta t + \sqrt{V_{t_{i-1}} \Delta t} W_1$$

and the variance process is given by;

$$V_{t_i} = V_{t_{i-1}} + \kappa(\theta - V_{t_{i-1}})\Delta t + \sigma \sqrt{V_{t_{i-1}} \Delta t} W_2$$

A large number of stock price paths are simulated over the life of the option, using the stochastic process $S_t$. For each stock price path, the terminal price and the value of the option at the terminal price are obtained, and the option value discounted back to time zero at the risk-free rate. This produces the option price for one path. This process is repeated many times, and the price of the option is taken as the mean of the option price of each path. It is expensive to use Monte Carlo due to the large number of time steps required to achieve convergence with this discretization.

An issue arising from this model is the fact that the normally distributed Brownian motion increments may give rise to negative values of $V_t$ . To deal with this problem, practitioners have generally adopted one of two approaches. Either the absorbing assumption: If $V_{t_{i-1}} < 0$ then $V_{t_{i-1}} = 0$, or the reflecting assumption: If $V_{t_{i-1}} < 0$ then $V_{t_{i-1}} = -V_{t_{i-1}}$.

### 7.2.1 Milstein Discretization

For our purposes of pricing barrier options, we have used Milstein discretization. By going to one higher order in the Itô-Taylor expansion of $V(t + \Delta t)$, we arrive at the following discretization of the variance process:

$$V_{t_i} = V_{t_{i-1}} + \kappa(\theta - \frac{V_{t_{i-1}}}{2})\Delta t + \sigma \sqrt{V_{t_{i-1}} \Delta t} W_2 + \frac{\sigma^2}{4}\Delta t(W_2^2 - 1)$$

This can be written as

$$V_{t_i} = (\sqrt{V_{t_{i-1}}} + \frac{\sigma^2}{2}\sqrt{\Delta t}W_2)^2 + \kappa(\theta - V_{t_{i-1}})\Delta t \frac{\sigma^2}{4}\Delta t$$

We note that if $V_{t_i} > 0$ and $4\lambda\theta/\sigma^2 > 1$, the variance process is positive. However this does not carry over to the discretization and negative variances must be watched as stipulated above.

When simulating Bates model the asset equation takes the following form

$$x_{t_i} = x_{t_{i-1}} + (r - \frac{V_{t_{i-1}}}{2})\Delta t + \sqrt{V_{t_{i-1}}\Delta t}W_1 + J_t X_t$$
$$V_{t_i} = (\sqrt{V_{t_{i-1}}} + \frac{\sigma^2}{2}\sqrt{\Delta t}W_2)^2 + \kappa(\theta - V_{t_{i-1}})\Delta t \frac{\sigma^2}{4}\Delta t$$

where $dX_t$ is a Poisson counter with intensity $\lambda$ and is simulated as $Pr(X_t = 1) = \lambda dt$ and $Pr(X_t = 0) = 1 - \lambda dt$. The jumps size $J_t$ is log-normally distributed and is depicted as:

$$\frac{\log(1 + J_t) - \log(1 + \mu_j) + \sigma_j^2/2}{\sigma_j} \sim N(0, 1)$$

If we let $U_t$ be a normally distributed variable, then we can simulate the jumps size through:

$$J_t = \exp\left(\sigma_j U_t + \log(1 + \mu_j) - \frac{\sigma^2}{2}\right) - 1$$

## 7.3 Exact Simulation Model for Option Pricing

Broadie and Kaya [5] suggest an exact simulation method for the Heston model which would solve the issue of having negative values of $V_t$. However this method is time consuming and complicated to implement, as it involves integration of a characteristic function expressed in terms of Bessel functions. We outline the process followed for completeness.

The stock price at time $t$, given the values of $S_u$ and $V_u$ for $u < t$ , are given as:

$$S_t = S_u \exp\left[r(t-u) - 0.5\int_u^t V_s ds + \rho\int_u^t \sqrt{V_s}dW_s^{(1)} + \sqrt{1-\rho^2}\int_u^t \sqrt{V_s}dW_s^{(2)}\right] \tag{7.1}$$

and the variance at time $t$ is given by the equation:

$$V_t = V_u + \kappa\theta(t-u) - \kappa\int_u^t V_s ds + \sigma_v \int \sqrt{V_s}dW_s^{(1)} \tag{7.2}$$

The following steps are followed to sample from the distribution of $(S_t, V_t)$

- Generate a sample from the distribution of $V_t$ given $V_u$
- Generate a sample from the distribution of $\int_u^t V_s ds$ given $V_t$ and $V_u$
- Recover $\int_u^t \sqrt{V_s} dW_s^{(1)}$ from 7.1 given $V_t$ , $V_u$ and $\int_u^t V_s ds$
- Generate a sample from the distribution of $S_t$ given $\int_u^t \sqrt{V_s} dW_s^{(1)}$ and $\int_u^t \sqrt{V_s} ds$

## 7.4 Implementing Barrier Options

### 7.4.1 Monte Carlo Pricing

Under Monte Carlo we used Milstein discretization to simulate the paths of the stock price and variance processes under both the Heston and Bates model. For both models we use a time step of $dt = 1/252$, which would correspond to one trading day and with 1,000,000 simulations. The strike $K$ is taken as equal to spot $S_0$. From the results one can check that the barrier results agree well with the identity DIB + DOB = vanilla call = UIB + UOB. In addition, we generated the stock process under the Black Scholes model. This was to compare the impact of stochastic volatility with that of a constant volatility in pricing barrier options.

### 7.4.2 Binomial Tree

Like most path-dependent options, barrier options can be priced via a binomial tree. The paper by Cox, Ross & Rubinstein [10] introduces the binomial method and this has since been adapted to various other option types such as barrier options. We use a binomial tree so as to compare price results with those generated using Monte Carlo methods.

The up and down movements of barrier options under the binomial method remain the same, such that

$$u = e^{\sigma\sqrt{T-t}}$$
$$d = e^{-\sigma\sqrt{T-t}}$$

this can be reduced to

$$d = \frac{1}{u}$$

and the probability of an up and down movements are respectively given as

$$p_u = \frac{e^{(r-d)(T-t)} - d}{u - d}$$
$$p_d = 1 - p_u$$

An important point to note with regards to barrier option pricing when using a binomial tree is the fact that with the existence of barriers, the “zig-zag” movements of a binomial model will create a challenge, as the true barrier is not the same barrier implied by the tree. This is because the binomial tree places the barriers at node points.

Various solutions have been suggested. Hull [18] illustrates this by considering an inner barrier and an outer barrier, between which lies the true barrier. For our purposes we consider an alternative solution by Boyle & Lau [4]. Boyle and Lau suggest a way to determine which nodes will give good approximate pricing of a barrier option. The number of time steps which will give the most accurate prices when using the binomial lattice is given as:

$$\text{Node}(m) = \frac{m^2\sigma^2 T}{[\ln \frac{S}{H}]^2} \tag{7.3}$$

where H is the barrier level and $m$ is equal to $1, 2, 3.., n$ nodes. Although these optimal nodes will provide a more accurate value for the barrier, a large number of time steps should be used to determine a reasonable value [16].

## 7.5 Numerical Results

We begin by looking at the pricing of European call option using Heston's volatility model and the Bates model. The results are then compared to Monte Carlo. Finally, we present barrier option prices simulated using Monte Carlo under both the Heston and Bates model.

### 7.5.1 Heston SV Model and Bates SVJ Model Using Fourier Transform

The results for European call options are presented in this section. Table 3 gives the values of the Heston parameters used for pricing.

Table 3: Estimated Parameters.

| Parameter | Heston | Bates |
|---|---|---|
| S | 100 | 100 |
| T | 1 | 1 |
| r | 3 % | 3% |
| $\rho$ | -0.9535 | -0.7916 |
| $\theta$ | 0.0936 | 0.1049 |
| $\kappa$ | 2.1689 | 3.4412 |
| $\sigma_v$ | 0.3309 | 0.4529 |
| $V_0$ | 0.1123 | 0.0889 |
| $\lambda$ | | 0.0837 |
| $\mu$ | | 0.0779 |
| $\delta$ | | 0.0720 |

Tables 4, 5 and 6 gives the Simulation results obtained for maturities T = 0.5, 1, 5 and 10 using the parameters above. This results are compared to Monte Carlo Simulation and are presented here as a check that the models produce adequate results across all maturities and strikes.

In the case of the Heston model, we made mention of the COS method as an alternative to quadrature integration techniques when using Fourier transform methods (referred to here as FT). We have implemented the Heston Model using both methods for comparison purposes and included results using Monte Carlo simulations.

Table 4: Comparison of the Fourier Transform, COS and Monte Carlo simulation for European call option with time to maturity T = 0.5 ,T = 1 year

| Heston Volatility Model | | | | | | |
|---|---|---|---|---|---|---|
| Strike | T = 0.5 | | | T = 1 | | |
| K | FT | COS | MC | FT | COS | MC |
| 50 | 50.7385 | 50.7997 | 50.8226 | 51.8109 | 51.8121 | 51.9123 |
| 75 | 27.4140 | 27.4149 | 27.5221 | 30.0697 | 30.0684 | 30.2286 |
| 100 | 9.6614 | 9.6619 | 9.6889 | 13.6891 | 13.6899 | 13.5238 |
| 125 | 1.5443 | 1.5554 | 1.2918 | 4.4060 | 4.4072 | 3.8896 |
| 150 | 0.0499 | 0.0517 | 0.0127 | 0.8563 | 0.8577 | 0.4970 |

Table 5: Comparison of the Fourier Transform, COS and Monte Carlo simulation for European call option with time to maturity T = 5 ,T = 10 years

| Heston Volatility Model | | | | | | |
|---|---|---|---|---|---|---|
| Strike | T = 5 | | | T = 10 | | |
| K | FT | COS | MC | FT | COS | MC |
| 50 | 59.8633 | 59.8640 | 59.8406 | 67.7224 | 67.7230 | 67.8728 |
| 75 | 44.2943 | 44.2983 | 44.2883 | 55.8840 | 55.8851 | 55.6726 |
| 100 | 32.1754 | 32.1744 | 32.0960 | 46.3524 | 46.3521 | 46.3543 |
| 125 | 23.0439 | 23.0455 | 23.0801 | 38.6457 | 38.6454 | 38.6557 |
| 150 | 16.3256 | 16.3251 | 16.2834 | 32.3796 | 32.3821 | 32.2892 |

The Heston volatility model which we described in chapter 6 using Fourier transform produces satisfactory results. The COS method comapares well with the FT method, with results similar to two decimal places. Both call option prices are well in line with the Monte Carlo results to atleast one decimal point across all maturities and across the various strike prices.

Table 6: Comparison of the Bates model and Monte Carlo simulation for European call option with time to maturity T = 0.5 ,1, 5 and 10 years.

| Bates Stochastic Volatility and Jump Diffusion Model | | | | | | | | |
|---|---|---|---|---|---|---|---|---|
| Strike | T = 0.5 | | T = 1 | | T = 5 | | T = 10 | |
| K | FT | MC | Fourier | MC | FT | MC | FT | MC |
| 50 | 50.7876 | 50.7818 | 51.7718 | 51.7297 | 60.0631 | 60.1021 | 68.2008 | 68.2054 |
| 75 | 27.2561 | 27.2456 | 29.9332 | 29.9992 | 44.8915 | 44.8272 | 56.8354 | 56.8584 |
| 100 | 9.2662 | 9.3422 | 13.6043 | 13.6810 | 32.2049 | 32.3362 | 47.7584 | 47.8294 |
| 125 | 1.3619 | 1.4857 | 4.5211 | 4.6143 | 24.4365 | 24.6356 | 40.4380 | 40.5413 |
| 150 | 0.0378 | 0.0917 | 1.0212 | 1.1309 | 17.9406 | 18.0784 | 34.4865 | 34.4948 |

Similarly the Bates model produces satisfactory results. The call option prices are well in line with the Monte Carlo results to at least one decimal point across all maturities and across the various strike prices.

### 7.5.2 Barrier Option Prices

We present barrier option prices simulated using Monte Carlo simulations. The strike price is the same as the stock price set at 6689.95. The risk free rate is constant at 3% and time to maturity is 1 year. Paths generated are 1,000,000 with a time step of 1/252. BS is the Black Scholes model and B&L BT is the Boyle and Lau binomial tree model.

Table 7 depicts results for knock-out call options.

| Barrier Option Prices | | | | | | | | |
|---|---|---|---|---|---|---|---|---|
| | Down-Out | | | | Down-In | | | |
| Barrier (H) | SV | SVJ | BS | B&L BT | SV | SVJ | BS | B&L BT |
| $0.5S_0$ | 916.9209 | 916.5659 | 913.0902 | 914.5558 | 0.0179 | 0.0224 | 0.0001 | 0.0011 |
| $0.6S_0$ | 915.7544 | 915.2319 | 913.0893 | 913.9105 | 0.7261 | 0.8397 | 0.2043 | 0.1973 |
| $0.7S_0$ | 905.5508 | 905.9896 | 906.2436 | 908.6395 | 10.9163 | 10.6891 | 6.5816 | 6.2504 |
| $0.8S_0$ | 842.0932 | 843.5802 | 850.5823 | 852.6524 | 74.3071 | 72.4924 | 46.7810 | 73.1332 |
| $0.9S_0$ | 618.6059 | 620.0832 | 626.1130 | 624.6526 | 297.6513 | 296.3469 | 288.1806 | 290.2013 |

Table 8 depicts knock-in call options.

| Barrier Option Prices | | | | | | | | |
|---|---|---|---|---|---|---|---|---|
| | Up-Out | | | | Up-In | | | |
| Barrier (H) | SV | SVJ | BS | B&L BT | SV | SVJ | BS | B&L BT |
| $1.1S_0$ | 4.7306 | 4.9383 | 3.4580 | 3.3110 | 911.4312 | 912.0493 | 912.5857 | 910.8205 |
| $1.2S_0$ | 47.7760 | 47.2918 | 32.7089 | 32.1707 | 869.1767 | 869.3904 | 882.4158 | 881.9323 |
| $1.3\mathrm{S}_0$ | 159.7381 | 153.5373 | 105.2039 | 104.9202 | 756.8370 | 763.1867 | 811.2977 | 809.1907 |
| $1.4S_0$ | 329.6156 | 310.0022 | 213.6308 | 213.9091 | 586.6267 | 606.8593 | 701.7497 | 700.2196 |
| $1.5S_0$ | 519.4026 | 479.9235 | 338.6768 | 339.2094 | 397.3655 | 437.8745 | 574.8627 | 575.6705 |

Under the SV and SVJ models, one can check that the barrier results agree well with the identity DIB + DOB = vanilla call = UIB + UOB. This suggests that the simulation results converge relatively well. The prices of the SV and SVJ model are similar in magnitude in most instances, except for options which are at 40% above the stock price in both the up-and-in barrier options and up-and-out barrier options.

In comparison to the Black Scholes and binomial tree results, we observe that the calculated vanilla call prices for the SV and SVJ models remain relatively similar. In the case of the DIC we note that for barriers below 80% of the spot price, the BS and BT results are lower than those of the corresponding stochastic volatility models.

This may be explained by the fact that stochastic volatility will introduce a higher probability of the stock price breaching the barrier far below the spot price. This can be observed in the probabilities shown in Appendix C. The relationship DO + DI = call price implies that if there is a difference in the price between down-and-in options, then we can expect a corresponding reverse price difference in the down-and-out options between the BS/BT prices and the those of the stochastic volatility model.

In the case of UOC and UIC, we note that the BS/BT results for the UIC are significantly higher than those of corresponding SV and SVJ models for barriers above 30% of the spot price. The probabilities in Appendix C reveals that there is a higher probability that the upper barrier is breached in the binomial tree compared to the stochastic volatility models. Given that the UOC options of the binomial tree are given by the relationship vanilla call = UIB + UOB then we observe that the corresponding prices are lower than those of the SV and SVJ models.

# 8 Conclusion

In this paper we explored the implementation of the Heston and Bates models. The empirical results using DAX options data show that stochastic volatility models achieve a relatively close fit to the vanilla market especially for medium to long term maturities. However, including jumps to the SV model fits shorter maturities better than the stochastic volatility model alone. This is best observed using the graph depicting the difference between implied volatility and market volatilities, where we observe smaller differences for shorter maturities when jumps are incorporated.

We note that call option prices by both Heston and Bates model yield similar results with respect to vanilla options using Fourier transform and using Monte Carlo simulations. Barrier option prices modeled with both Heston and Bates model using Monte Carlo simulation are very similar across the various maturities and strikes. However, for barrier levels far from the spot prices, there seems to be a slightly bigger price difference for the knock-in options. Equally the binomial tree yields barrier option prices that differ from the stochastic volatility models, although pricing vanilla options under these models yields similar prices. This may be due to the fact that the stochastic volatility models give rise to a skewed distribution of future spot prices which may result in higher probabilities of breaching low barriers and lower probabilities of breaching high barriers. We note that for barrier levels close to the spot price, the prices under the stochastic volatility models, Black Scholes and using a binomial tree are in most cases of similar magnitude.

# A Option Pricing formula for the Black Scholes Model

In the Black Scholes model, the stock price process is assumed to follow a geometric Brownian motion

$$dS_t = \mu S_t dt + \sigma S_t dW \tag{A.1}$$

Suppose that $V$ is the price of a call option or other derivative contingent on S. The variable $V$ must be some function of S and t. Hence by Ito's lemma

$$dV = \left(\frac{\partial V}{\partial S}\mu S + \frac{\partial V}{\partial t} + \frac{1}{2}\frac{\partial^2 V}{\partial S^2}\sigma^2 S^2\right)dt + \frac{\partial V}{\partial S}\sigma S dW \tag{A.2}$$

Next we set up a portfolio consisting of a short position in a call option and a long position of $\Delta$ units of stock. Define $\Pi$ as the value of the portfolio

$$\Pi = -V + \Delta S \tag{A.3}$$

The change in the value of this portfolio in a small time interval is given by

$$d\Pi = dV + \Delta dS \tag{A.4}$$

substituting equations A.1 and A.2 into A.4 gives

$$\begin{aligned} d\Pi &= -\left(\frac{\partial V}{\partial S}\mu S + \frac{\partial V}{\partial t} + \frac{1}{2}\frac{\partial^2 V}{\partial S^2}\sigma^2 S^2\right)dt - \frac{\partial V}{\partial S}\sigma S dz + \Delta\mu S dt + \Delta\sigma S dW \\ &= \left( - \frac{\partial V}{\partial S}\mu S - \frac{\partial V}{\partial t} - \frac{1}{2}\frac{\partial^2 V}{\partial S^2}\sigma^2 S^2 + \Delta\mu S\right)dt \\ &\quad + \left( - \frac{\partial V}{\partial S}\sigma S + \Delta\sigma S\right)dW \end{aligned} \tag{A.5}$$

To make the portfolio riskless, we choose $\delta = \frac{\partial V}{\partial S}$. Then

$$d\Pi = \left( - \frac{\partial V}{\partial t} - \frac{1}{2}\frac{\partial^2 V}{\partial S^2}\sigma^2 S^2\right)dt \tag{A.6}$$

In the absence of arbitrage opportunities, the riskless portfolio must earn a risk-free rate $r$, such that

$$d\Pi = r\Pi dt \tag{A.7}$$

Substituting equations A.3 and A.6 into A.7, this becomes

$$\left( - \frac{\partial V}{\partial t} - \frac{1}{2}\frac{\partial^2 V}{\partial S^2}\sigma^2 S^2\right)dt = r\left( - V + \frac{\partial V}{\partial S}S\right)dt \tag{A.8}$$

or

$$\frac{\partial V}{\partial t} + rS\frac{\partial V}{\partial S} + \frac{1}{2}\sigma^2 S^2 \frac{\partial^2 V}{\partial S^2} = rV \tag{A.9}$$

Equation A.9 is the Black Scholes partial differential equation.

# B Option Pricing formula for the Heston Stochastic Model

This section we follow Wilmott [30] closely. Suppose that the stock price $S$ and its variance $\nu$ satisfy the following SDE

$$dS_t = \mu_t S_t dt + \sqrt{\nu}\sigma S_t dW_1$$

$$d\nu_t = \alpha(S_t, \nu_t, t)dt + \eta\beta(S_t, \nu_t, t)\sqrt{\nu_t}dW_2$$

with

$$\langle dW_1 dW_2 \rangle = \rho dt$$

where $\mu_t$ is the (deterministic) instantaneous drift of stock price returns, $\eta$ is the volatility of volatility and $\rho$ is the correlation between random stock price returns and changes in $\nu_t$. $dW_1$ and $dW_2$ are Weiner processes. In the Black Scholes case, there is only one source of randomness, the stock price, which can be hedged with stock. In the present case, the random changes in volatility also need to be hedged in order to form a risk-less portfolio. So we set up a portfolio $\Pi$ containing the option being prices whose value we denote by $V(S, \nu, t)$ a quantity $-\Delta$ of the stock and a quantity $-\Delta_1$ of another asset whose value $V_1$ depends on volatility. We have

$$\Pi = V + \Delta S - \Delta_1 V_1$$

The change in the value of this portfolio in a small time interval is given by

$$\begin{aligned}
d\Pi = &\left\{ \frac{\partial V}{\partial t} + \frac{1}{2}\nu S^2 \frac{\partial^2 V}{\partial S^2} + \rho\eta\nu\beta S \frac{\partial^2 V}{\partial \nu \partial S} + \frac{1}{2}\eta^2\nu\beta^2 \frac{\partial^2 V}{\partial \nu^2} \right\} dt \\
&-\Delta_1 \left\{ \frac{\partial V_1}{\partial t} + \frac{1}{2}\nu S^2 \frac{\partial^2 V_1}{\partial S^2} + \rho\eta\nu\beta S \frac{\partial^2 V_1}{\partial \nu \partial S} + \frac{1}{2}\eta^2\nu\beta^2 \frac{\partial^2 V_1}{\partial \nu^2} \right\} dt \\
&+\left\{ \frac{\partial V}{\partial S} - \Delta_1 \frac{\partial V_1}{\partial S} - \Delta \right\} dS \\
&+\left\{ \frac{\partial V}{\partial \nu} - \Delta_1 \frac{\partial V_1}{\partial \nu} \right\} d\nu
\end{aligned}$$

To make the portfolio riskless, we choose

$$\frac{\partial V}{\partial S} - \Delta_1 \frac{\partial V_1}{\partial S} - \Delta = 0$$

to eliminate $dS$ terms, and

$$\frac{\partial V}{\partial \nu} - \Delta_1 \frac{\partial V_1}{\partial \nu} = 0$$

to eliminate $d\nu$ terms. This leaves us with

$$\begin{aligned}
d\Pi &= \left\{ \frac{\partial V}{\partial t} + \frac{1}{2}\nu S^2 \frac{\partial^2 V}{\partial S^2} + \rho\eta\nu\beta S \frac{\partial^2 V}{\partial \nu \partial S} + \frac{1}{2}\eta^2 \nu \beta^2 \frac{\partial^2 V}{\partial \nu^2} \right\} dt \\
&\quad - \Delta_1 \left\{ \frac{\partial V_1}{\partial t} + \frac{1}{2}\nu S^2 \frac{\partial^2 V_1}{\partial S^2} + \rho\eta\nu\beta S \frac{\partial^2 V_1}{\partial \nu \partial S} + \frac{1}{2}\eta^2 \nu \beta^2 \frac{\partial^2 V_1}{\partial \nu^2} \right\} dt \\
&= r\Pi dt \\
&= r(V - \Delta S - \Delta_1 V_1) dt
\end{aligned}$$

where we have used the fact that the return on a risk-free portfolio must equal the risk-free rate $r$ which we will assume to be deterministic for our purposes. Collecting all $V$ terms on the left-hand side and all $V_1$ terms on the right-hand side, we get

$$\begin{aligned}
& \frac{\frac{\partial V}{\partial t} + \frac{1}{2}\nu S^2 \frac{\partial^2 V}{\partial S^2} + \frac{1}{2}\eta^2 \nu \beta^2 \frac{\partial^2 V}{\partial \nu^2} + rS\frac{\partial V}{\partial S} - rV}{\frac{\partial V}{\partial \nu}} \\
= & \frac{\frac{\partial V_1}{\partial t} + \frac{1}{2}\nu S^2 \frac{\partial^2 V_1}{\partial S^2} + \rho\eta\nu\beta S \frac{\partial^2 V_1}{\partial \nu \partial S} + \frac{1}{2}\eta^2 \nu \beta^2 \frac{\partial^2 V_1}{\partial \nu^2} + rS\frac{\partial V_1}{\partial S} - rV_1}{\frac{\partial V_1}{\partial \nu}}
\end{aligned}$$

The left-hand side is a function of $V$ only and the right-hand side is a function of $V_1$ only. The only way that this can be is for both sides to equal to some function $f$ of the independent variables $S$, $\nu$ and $t$. We deduce that

$$\begin{aligned}
& \frac{\partial V}{\partial t} + \frac{1}{2}\nu S^2 \frac{\partial^2 V}{\partial S^2} + \rho\eta\nu\beta S \frac{\partial^2 V}{\partial \nu \partial S} + \frac{1}{2}\eta^2 \nu \beta^2 \frac{\partial^2 V}{\partial \nu^2} + rS\frac{\partial V}{\partial S} - rV \\
= & -(\alpha - \phi\beta\sqrt{\nu})\frac{\partial V}{\partial \nu}
\end{aligned}$$

where, without loss of generality, we have written the arbitrary function $f$ of $S$, $\nu$ and $t$ as $(\alpha - \phi\beta\sqrt{\nu})$, where $\alpha$ and $\beta$ are the drift and volatility functions from the SDE (B.1) for instantaneous variance.

# C Barrier Option Probabilities

The table summarizes the probabilities that the spot price breaches the respective barriers using various model.

| Barrier Option Probabilities | | | |
|---|---|---|---|
| Barrier (H) | BS | SV | SVJ |
| $0.5S_0$ | 2.58% | 7.09% | 6.73% |
| $0.6S_0$ | 10.12% | 15.47% | 15.09% |
| $0.7S_0$ | 25.29% | 28.93% | 28.41% |
| $0.8S_0$ | 46.78% | 47.17% | 47.17% |
| $0.9S_0$ | 72.11% | 70.09% | 70.51% |
| | | | |
| $1.1S_0$ | 71.56% | 72.95% | 72.39% |
| $1.2S_0$ | 51.71% | 51.80% | 51.53% |
| 1.3S$_0$ | 35.85% | 34.30% | 34.42% |
| $1.4S_0$ | 24.53% | 20.98% | 21.63% |
| $1.5S_0$ | 16.50% | 11.69% | 12.75% |

# References

[1] Alan l. Lewis., (2001), A Simple Option Formula For general Jump Diffusion And Other Exponential Lĕvy Processes. manuscript, Envision Financial Systems and OptionCity.net, Newport Beach, California, USA, 2001. Available at http://optioncity.net/pubs/ExpLevy.pdf.

[2] Artur Sepp, (2003), Fourier Transform for option Pricing under Affine Jump-Diffusions: An Overview. Available at www.hot.ee/seppar.

[3] Bates D., (1996), Jump and Stochastic Volatility: Exchange rate Processes Implicit in Deutshe mark in Options, review of Financial Studies, Vol.9, pp.69-107.

[4] Boyle, P., & Lau, S.H., (1994), Bumping Against the Barrier with the Binomial Method, Journal of Derivatives, 1, pp.6-14.

[5] Broadie, M., and Ö. Kaya,(2004), Exact Simulation of Stochastic Volatility and other Affine Jump Diffusion Processes. Operations Research, Vol.54(2), pp.217-231.

[6] Carr, P. and Madan, D. B. (1999), Option evaluation using fast fourier transform, Journal of Computational Finance 2(4), pp.61-73.

[7] Christian Kahl and Peter Jäckel., (2005), Not-so-complex Logarithms in Heston Model. Wilmott Magazine, Vol.19, pp.94-103.

[8] Cox, J.C., Ingersoll, J.E., and Ross, S.A., (1985), A theory of the term structure of interest rates, Econometrica, Vol.53, No.2, pp.385-407.

[9] Cox, J.C. and Ross, S.A., (1976), The Valuation of Options for Alternative Stochastic Processes, J. Fin. Economics, Vol.31, pp.383-402.

[10] Cox, J., Ross, S. and Rubinstein M. (1979), Option Pricing: A Simplified Approach. Journal of Financial Economics, 7.

[11] Duffie, D. and Glynn, P., (1995), Efficient Monte Carlo Estimation of Security Prices, The Annals of Applied Probability, Vol.4, No.5, pp.897-905.

[12] Duffie D, Pan J, and K Singleton, (2000), Transform analysis and asset pricing for affine jump-diffusion, Econometrica, Vol.68, No.6, pp.1343-1376.

[13] Eraker B, Johannes M, and N Polson, (2003), The Impact of Jumps in Volatility and Returns, Journal of Finance, Vol.58, No.3.

[14] Fang H, (2000), Option Pricing Implications of a Stochastic Jump Rate, University of Virginia.

[15] Fang, F. and Oosterlee, (2008) C.W. A novel option pricing method based on Fourier-cosine series expansions, submitted, see http://ta.twi.tudelft.nl/mf/users/oosterle/oosterlee/COS.pdf.

[16] www.global-derivatives.com/index.php/pricing-models-topmenu-37/13#ClosedForm.

[17] Heston S., (1993), A Closed-Form Solution of Options with Stochastic Volatility with Applications to Bond and Currency Options, Review of Financial Studies, Vol.6, No.2, pp.327-343.

[18] Hull, J., Options, Futures & Other Derivatives, 5th Edition 2002.

[19] Hull, J., and White, A., (1987), The Pricing of Options with Stochastic Volatilities. Journal of Finance, Vol.42, pp.281-300.

[20] Jian Wang, (2007), Convexity of option prices in the Heston model, U.U.D.M. Project Report. Available at http://uu.diva-portal.org/smash/record.jsf?pid=diva2:304668.

[21] Jim Gatheral, The Volatility Surface, A Practitioners Guide.

[22] Kou S.G., (2002), A jump diffusion model for option pricing, Management Science Vol.48, pp.1086-1101.

[23] Merton, R. C., (1976), Option pricing when underlying stock returns are discontinuous. J. Financial Economy. Vol.3, pp.125-144.

[24] Maheu J and T McCurdy, (2004), News Arrival, Jump Dynamics, and Volatility Components for Individual Stock Returns, Journal of Finance, Vol.54, No.2.

[25] Reuters. Available at www.reuters.com/.

[26] Scott L.O., (1997), Pricing Stock Options in a Jump-Diffusion Model with Stochastic Volatility and Interest Rates: Application of Fourier Inversion Methods, Mathematical Finance, Vol.7(4), pp.413-424.

[27] Schoutens, Wim, Erwin Simons and Jurgen Tistaert, (2004), A Perfect Calibration! Now What?, Wilmott Magazine 2, pp.66-78.

[28] Stein E. and Stein J., (1991), Stock Price Distributions with Stochastic Volatility, Review of Financial Studies, Vol.4, pp.727-752.

[29] Schobel R. and Zhu J., (1998), Stochastic Volatility With an OrnsteinUhlenbeck Process: An Extension. Available at http://papers.ssrn.com/sol3/papers.cfm?abstract-id=100831.

[30] Wilmott, Paul. (2000). Paul Wilmott on Quantitative Finance. Chichester: John Wiley & Sons.